https://doi.org/10.5194/egusphere-2025-635
Preprint. Discussion started: 21 February 2025

Airborne quantification of Angolan offshore oil and gas methane emissions

Alina Fiehn[1], Maximilian Eckl[1], Magdalena Pühl[1], Tiziana Bräuer[1], Klaus-Dirk Gottschaldt[1], Heinfried Aufmhoff[1], Lisa Eirenschmalz[1,2], Gregor Neumann[1], Felicitas Sakellariou[1], Daniel Sauer[1], Robert Baumann[1], Guilherme De Aguiar Ventura[3], Winne Nayole Cadete[3], Dario Luciano Zua[3], Manuel Xavier[4], Paulo Correia[4], Anke Roiger[1]

[1] Deutsches Zentrum für Luft- und Raumfahrt, Institut für Physik der Atmosphäre, Oberpfaffenhofen, Germany
[2] Deutsches Zentrum für Luft- und Raumfahrt, Flugexperimente, Oberpfaffenhofen, Germany
[3] Agência Nacional de Petróleo, Gás e Biocombustíveis, Luanda, Angola
[4] Ministério dos Recursos Minerais, Petróleo e Gás, Luanda, Angola

Correspondence to: Alina Fiehn (alina.fiehn@dlr.de)

Abstract. In September 2022, the METHANE-To-Go Africa (MTGA) scientific aircraft campaign, part of UNEP's International Methane Emissions Observatory (IMEO) Methane Science Studies, conducted the first methane (CH_4) emissions measurements from the offshore oil and gas sector in West Africa. This study provides the first independent empirical data on emissions in this previously unstudied region. Emissions from Angolan offshore facilities were quantified using an aircraft-based mass balance method, estimating total sector emissions and assessing 30 individual facilities and 10 facility groups.

Our findings show consistent emissions across different days for most facilities. However, high-emission events of 10 and 4 t h^{-1} were observed at two facilities, significantly impacting total emissions. Older, low-producing shallow-water facilities had higher emissions than newer, high-producing deep-water facilities. Production volume is a poor proxy for methane emissions; instead, facility age and maintenance status should be considered risk factors. However, due to variations in asset design and operation, regular measurements are essential, prioritizing high-risk facilities.

Total CH_4 emissions from Angolan offshore facilities were estimated at 16.9 ± 5.3 t h^{-1}, only 20-22% of EDGAR and CAMS inventory estimates but over twice the amount reported by operators. Additional trace gas measurements, including CO_2, CO, C_2H_6, SO_2, NOy, and aerosols, provided insights into CH_4 sources, primarily from fugitive emissions and venting rather than flaring or combustion. This study presents a unique dataset on CH_4 emissions, improving our understanding of offshore oil and gas emissions in this critical region.

https://doi.org/10.5194/egusphere-2025-635
Preprint. Discussion started: 21 February 2025

1 Introduction

Atmospheric methane (CH_4) concentrations have more than doubled since the beginning of the industrial age, making it the second most significant long-lived anthropogenic greenhouse gas after carbon dioxide (CO_2). The oil and gas (O&G) sectors are major contributors, accounting for approximately 22% of global anthropogenic CH_4 emissions.

The 2015 Paris Agreement of the United Nations Framework Convention on Climate Change (UNFCCC) aims at limiting the global warming to below 1.5°C (UNFCCC, 2015). With a global warming potential 80–83 times that of CO_2 over a 20-year time horizon, CH_4 is the second most important anthropogenic greenhouse gas after CO_2, contributing 16% to the effective radiative forcing of well-mixed greenhouse gases since 1750 (IPCC, 2023). Considering its short lifetime of around a decade, CH_4 presents a high potential for mitigation strategies aimed at achieving the UNFCCC Paris Agreement's goal to mitigate climate warming (Nisbet et al., 2019). Recently, Angola signed up to the Global Methane Pledge, aiming to cut global CH_4 emissions by at least 30% from 2020 levels by 2030 (European Commission, United States of America, 2021).

The O&G sectors have been estimated to account for 22% (18–27%) of global anthropogenic CH_4 emissions (bottom-up in 2017; Saunois et al., 2020). Approximately 30% of global O&G production occurs offshore (IEA World Energy Outlook). This includes significant contributions from major offshore producing regions, such as the Gulf of Mexico, the North Sea, Brazil, West Africa, and Southeast Asia. CH_4 is emitted during routine operations on offshore O&G platforms for safety and operational reasons (e.g., shutdown or start-up of equipment during production) by either controlled venting or flaring. In the latter case, CO_2 is released simultaneously, with the CH_4 to CO_2 emission ratio dependent on the flaring efficiency. Another source of methane emission are unintended leaks on O&G installations.

Several studies indicate that bottom-up inventories underestimate emissions from the O&G industry (Schwietzke et al., 2016; Saunois et al., 2020; MacKay et al., 2021; Gorchov Negron et al., 2023). Unintended leaks as well as blow-outs can significantly contribute to CH_4 emissions (Lyon et al., 2015; Conley et al., 2016; Zavala-Araiza et al., 2017; Lee et al., 2018; Pandey et al., 2019; Varon et al., 2019). Top-down emission estimates from direct measurements close to sources can help to independently validate bottom-up estimates in inventory data. Better understanding, monitoring, and verification of CH_4 emissions associated with O&G operations are crucial parts of the Global Methane Pledge (European Commission and United States of America, 2021).

Emissions from offshore O&G facilities are especially uncertain. Observations are sparse, partly because offshore facilities are less accessible, but also because the satellite detection and quantification of offshore methane plumes are highly challenging due to the low albedo of the ocean surface in the relevant wavelengths. Therefore, only the biggest plumes are detected and only during favorable weather conditions. The smallest plume detected so far by satellite in offshore Angola is 0.8 t h^{-1} (UNEP, 2024). Airborne in-situ mass balance is currently the most reliable technique for assessing offshore methane emissions, because it has a low detection limit, good spatial coverage and can also be conducted under cloudy conditions.

Africa is a significant player in the global O&G industry, with major CH_4 emissions arising from the extraction and processing of these resources. Nigeria and Angola are the top producers of oil and natural gas in West Africa, with most of the production

https://doi.org/10.5194/egusphere-2025-635
Preprint. Discussion started: 21 February 2025

occurring offshore. The O&G sectors in Angola are a critical part of the country's economy and a significant player in the global energy market. A majority of Angola's oil production comes from offshore platforms. The country's offshore oil production is split between older shallow-water platforms closer to the coast and newer deep-water and ultradeep-water fields off the coast. These are tethered Floating Production Storage and Offloading (FPSO) vessels that can serve several oil fields at once and therefore have higher production volumes than the shallow-water platforms. A lot of the produced natural gas is associated gas from oil fields, and a significant portion is reinjected into reservoirs to enhance oil recovery. The FPSOs are connected to an underwater pipeline system that carries the associated gas to the operational LNG (liquefied natural gas) plant on the coast, where the gas is processed for export. The older facilities are not connected to this pipeline system.

Methane emissions from Angola's O&G sector are significant due to the nature of O&G extraction and processing activities. These emissions primarily originate from fugitive emissions, which are unintentional leaks from equipment and infrastructure; venting, which involves the intentional release of gas often due to safety reasons or the lack of infrastructure to capture and utilize associated gas; and flaring, which is the burning of excess gas that cannot be processed or sold.

Studies on CH_4 emission measurements from offshore platforms are limited but critical for accurate assessments. Some measurements have been conducted, such as ship-based measurements in the US Gulf of Mexico (Yacovitch et al., 2020), South-East Asia (Nara et al., 2014), and the North Sea (Hensen et al., 2019; Riddick et al., 2019).

In contrast to ship-based measurements, the mobility of aircraft allows for sampling of emission plumes both horizontally and vertically, providing more detailed information on marine boundary layer conditions. To date, airborne measurements around offshore facilities have been conducted in the Sureste Basin, Mexico (Zavala-Araiza et al., 2021), the US Gulf of Mexico (Gorchov Negron et al., 2023), the Norwegian Sea (Roiger et al., 2015; Foulds et al., 2022), and the North Sea (Cain et al., 2017; Lee et al., 2018; Pühl et al., 2024).

The METHANE-To-Go Africa (MTGA) campaign conducted the first airborne methane measurements in West Africa. The study provides an empirical understanding of the magnitude and location of CH_4 emissions from the O&G industry in Angola. This publication is structured as follows: In Section 2, we describe the data, including airborne observations, inventory data, operator reporting, and satellite data, as well as the mass balance method used for the processing of the airborne data. In Section 3, we compare the different emission estimates for individual facilities and the entire Angola offshore sector. Section 4 gives a Discussion and Summary.

2 Data and methods

The METHANE-To-Go project aims to better understand and quantify methane (CH_4) emissions from the O&G sector, with a focus on offshore exploration. Within the METHANE-To-Go series, which is financed by the International Methane Emissions Observatory (IMEO) of the United Nations Environment Programme (UNEP) and the German Aerospace Center (DLR), airborne studies covering Europe (Italy, Bosnia, Serbia), the coal mining in Poland and the Middle East O&G production were conducted. This study focuses on the exploration and production activities off the coast of Angola. The DLR Institute of Atmospheric Physics (IPA) conducted a measurement campaign during three weeks in September 2022 (Section

https://doi.org/10.5194/egusphere-2025-635
Preprint. Discussion started: 21 February 2025

2.1). Using an aircraft-based mass balance approach (Section 2.2) regional and facility-scale emissions are estimated. Results are compared to bottom-up emission inventories (Section 2.3), operator reporting (Section 2.4), and satellite data (Section 2.5).

2.1 Airborne observational data

The DLR Falcon research aircraft was instrumented with a comprehensive suite of in-situ measurement systems for the detection of methane and related trace gases and measurement flights were performed along the coastal regions of Gabon, the Congo, and Angola. The flight strategy was optimized for deriving regional estimates of different (sub-) regions. Quantification of facility-scale emissions was possible on most days due to very favorable weather conditions. The MTGA campaign with the DLR Falcon aircraft took place between 5 and 26 Sep 2022. The campaign base was in Libreville, Gabon, and 15 measurement flights with a total of 60 flight hours were conducted. For the 10 flights in Angola, we made refueling stops at Luanda airport. The Dassault Falcon 20E-5 (Registration: D-CMET) is a twin-engine jet with unique modifications. They include air inlets on the roof, four underwing hardpoints for particle measurements probes, in-situ instruments for trace gas measurements inside the cabin, and a nose boom for pressure measurement. When flying at low altitudes <300 m, the DLR Falcon has a ground speed of around 110 m s^{-1}, an endurance of 4 hours and can, thus, cover around 1,600 km during a single instrumented flight. Its instrumentation allows for precise meteorological measurements (Fimpel, 1991). High cabin temperatures of up to 50°C during the low-altitude low-speed measurement flights sometimes required improvisational cooling of some components, but in general the instrumentation worked well under the extreme conditions. Table 1 contains a list of the instruments installed and the parameters measured. Methane was measured with two instruments to provide redundancy for the primary target species of this campaign. We used the Quantum Cascade Laser Spectrometer (QCLS) methane data (Kostinek et al. (2019) for emission estimation and, if not available, the Picarro data (Dischl et al. (2024); Harlass et al. (2024) was used. A comparison of both instruments has shown good agreement within their measurement uncertainties. The additional trace gases provide further insights into the sources of CH_4 emissions, e.g. CO_2 helps to distinguish between flaring and fugitive/venting emissions.

Figure 1 shows the flight tracks of the 10 flights in Angola. Each region was covered by at least two, sometimes three flights. These were designed as either: 1.) survey, 2.) regional mass balance, 3.) or individual facility mass balance flights. The flight duration was around 4 hours with 1.5 hours used for the transfer to Libreville and Luanda and 2.5 hours spent in the measurement area. During this time between 6 and 18 facilities could be probed depending on their proximity.

https://doi.org/10.5194/egusphere-2025-635
Preprint. Discussion started: 21 February 2025

Table 1: Instrument overview for MTGA campaign on the DLR Falcon.

Instrument	Species/ Parameter	Measurement frequency	Measurement Technique	Reference
Aerodyne QCLS	CH_4, C_2H_6, $^{13}CH_4$, H_2O	0.5 s	Laser absorption spectroscopy	Kostinek et al. (2019)
Picarro G2401-m	CH_4, CO_2, H_2O	2 s	Cavity ring-down spectroscopy	Dischl et al. (2024); Harlass et al. (2024)
IT-CIMS	SO_2	1 s	Ion-trap chemical ionization mass spectrometry	Speidel et al. (2007)
Thermo SO2	SO_2	1 s	Pulsed fluorescence analyzer	Luke (1997)
ECO Physics TR	NO + NO_y	1 s	Chemiluminescence Technique	Harlass et al. (2024)
Aerosol	vol. and non-vol. particles	1s	Condensation Particle Counters and Thermodenuder	Feldpausch et al. (2006); Dischl et al. (2024)
MET package	3D-wind, temperature, humidity	10-100 Hz	5-hole pressure probe, PT100, dew point and Lyman-α	Fimpel (1991); Bramberger et al. (2017)

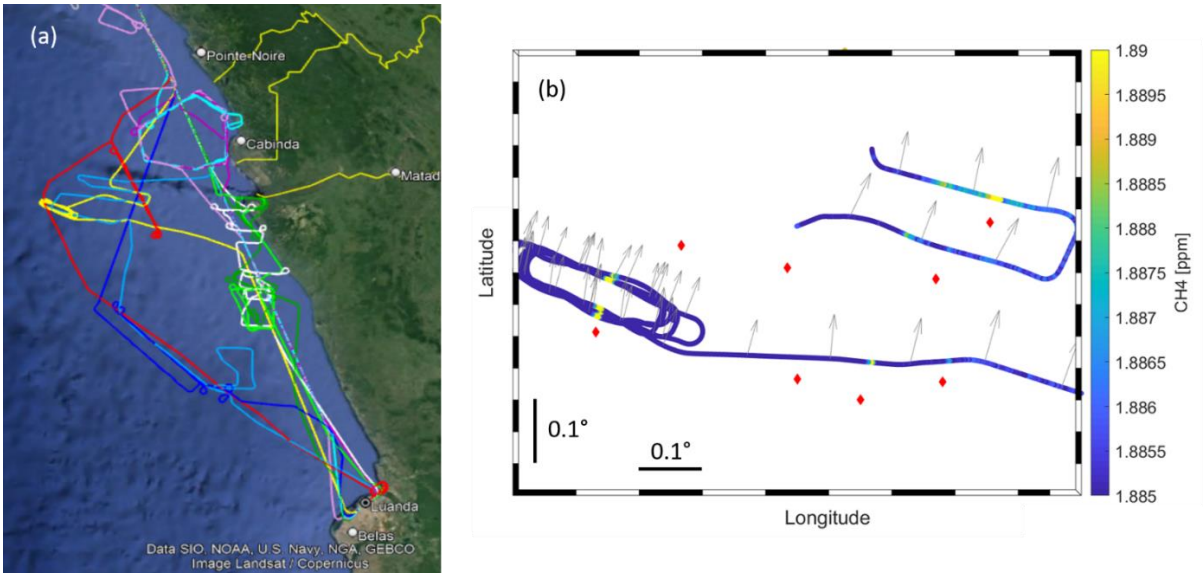

Figure 1: (a) Flight tracks of the 10 scientific flights during MTGA in Angola. (b) Map of CH_4 observations in the boundary layer from the yellow flight in (a). The flight track is color-coded with the observed CH_4 concentration. Latitude and longitude values are not specified to protect the anonymity of the operators. Red diamonds show the locations of facilities received from the operators and the arrows the measured wind direction. The facility in the west was sampled at 3.5 and 9 km distance and several altitudes using a racetrack pattern.

https://doi.org/10.5194/egusphere-2025-635
Preprint. Discussion started: 21 February 2025

2.2 Mass balance method

The emissions of facilities or groups of facilities are determined using the airborne mass balance method (Mays et al., 2009; Turnbull et al., 2011; Karion et al., 2013; Pitt et al., 2019; Fiehn et al., 2020; Pühl et al., 2024). In short, the balance between the in- and outflowing mass of an imaginary box around the target is the mass emitted inside the box. These emissions are transported downwind while turbulence spreads them horizontally and vertically until the plumes are well-mixed from the surface (in our case the ocean surface) up to the planetary boundary layer height (PBLH). The aircraft tracks constrain the sides of the box. The upwind side covers the inflow into the box and the downwind side is used to determine the outflow of the box. The flight patterns are designed to cover the box, and especially the downwind side at different altitudes, with the highest track right above the PBLH. The flight tracks should ideally be perpendicular to the wind direction with a distance of 5 to 10 km to the source region allowing for vertically well-mixed plumes (see below). There should also be sufficiently strong winds (>3 m s^{-1}) to rule out accumulations of the observed species in the box. For the calculation we make the following assumptions: First, the wind speed, wind direction, emissions, background concentrations and PBLH remain constant over the sampling time. Second, there is no entrainment/detrainment into the free troposphere. Third, the lifetime of the species is much longer than transport and sampling times, which is true for CH_4 (lifetime ~9 years) and other long-lived greenhouse gases. Finally, the trace gas plume is well-mixed between the lowest flight track and the ground. These criteria are most likely to be met in the early afternoon, when the PBLH has reached its maximum. The emissions F of all sources within the box are defined as the difference between inflow m_{in} and outflow mass fluxes m_{out}:

$$F = m_{out} - m_{in} = \sum_i (c_{out} - c_{in})\, v_{\perp,i}\, A_i \,. \qquad (1)$$

Here m_{out} of transect i is determined from the measured enhancement above background concentrations in the downwind transect c_{out}, the wind speed perpendicular to the transect $v_{\perp}$, and the area A_i of the downwind side of the box. m_{in} is the mass of gas going into the box calculated from the background concentration c_{in} in the upwind transect. Since we did not always measure in the upwind, the background concentrations are determined from the 20 s of measurement before and after the plume enhancement. The location of this time interval is selected manually after visual inspection of the measurement values. If a second plume is close to the target plume, only the interval before or after the target plume is used for background determination. Summing up the fluxes from all vertical transects i gives the mass flux through the entire plane. The concentration and wind observations between the flight transects at different altitudes are interpolated over the entire area of the outflow side. For interpolation we use the "layer"-method, which was also employed by Foulds et al. (2022), where the observed concentrations for each transect is assumed for the entire layer up to the middle between the next observation altitude. The lowest transect is extrapolated to the ground and the highest transect up to the PBLH assuming constant fluxes. We found no cases where the transect was still in the PBL, but no plume was detected any more, if it had been detected at lower altitudes. The uncertainty calculation and determination of the level of detection (LOD) is described in detail in Appendix A.

https://doi.org/10.5194/egusphere-2025-635
Preprint. Discussion started: 21 February 2025

Most flights were designed to deliver a regional emission estimate using the mass balance method. The Angolan facilities were grouped into regions according to geographical proximity for the flight execution. Each region was covered at least twice with survey or regional mass balance flights. At least one dedicated mass balance flight was done for each region. The coastal regions of Cabinda, Soyo and Angola were covered three times. Each measurement flight included vertical profiles to determine the PBLH before and after the downwind observations.

In general, the weather conditions were very favorable for mass balance calculations. This includes a clear boundary layer top and well-mixed plumes. The wind speed was stable throughout the measurements with a mean standard deviation of 0.36 m s^{-1}. The primary wind was southerly and around 5 m s^{-1}. This is visible in Figure 2a, which shows a map of one regional mass balance flight. The box pattern was slightly altered during the flight due to the plume being encountered further to the west than expected. All offshore facilities in the region were included in the mass balance box. The altitudes for the downwind transects were 220, 150, and 100 m, while the PBLH was at 350 m. Figure A2 shows example profiles of the variables through which the PBLH was estimated.

Some flights were designed as survey flights in order to scout all facilities of a region by flying a single transect downwind of the facilities, typically at an altitude in the middle of the PBL. Some parts of these flights also targeted a single facility with transects at different altitudes and distances using a racetrack pattern to get a thorough emission estimate. A combination of a survey flight with a racetrack pattern can be seen in Figure 1b. With both flight patterns we can determine the emissions of individual facilities. Estimating emissions from survey flights has a higher uncertainty than the racetrack, because the vertical extent of the plume is less certain. A case study for the transects of the racetrack in Figure 1b is shown in Appendix A.

Often the emissions of individual facilities or groups of facilities could be extracted from the regional mass balance flights. This was possible if a clear background was observed between two plumes and the wind was steady enough in the region to deduce the potential source installation for each plume. Facilities were grouped according to the plumes that could be separated from the measurements. An example of this is given in Figure 2 with the plumes of group 1 and group 2.

https://doi.org/10.5194/egusphere-2025-635
Preprint. Discussion started: 21 February 2025

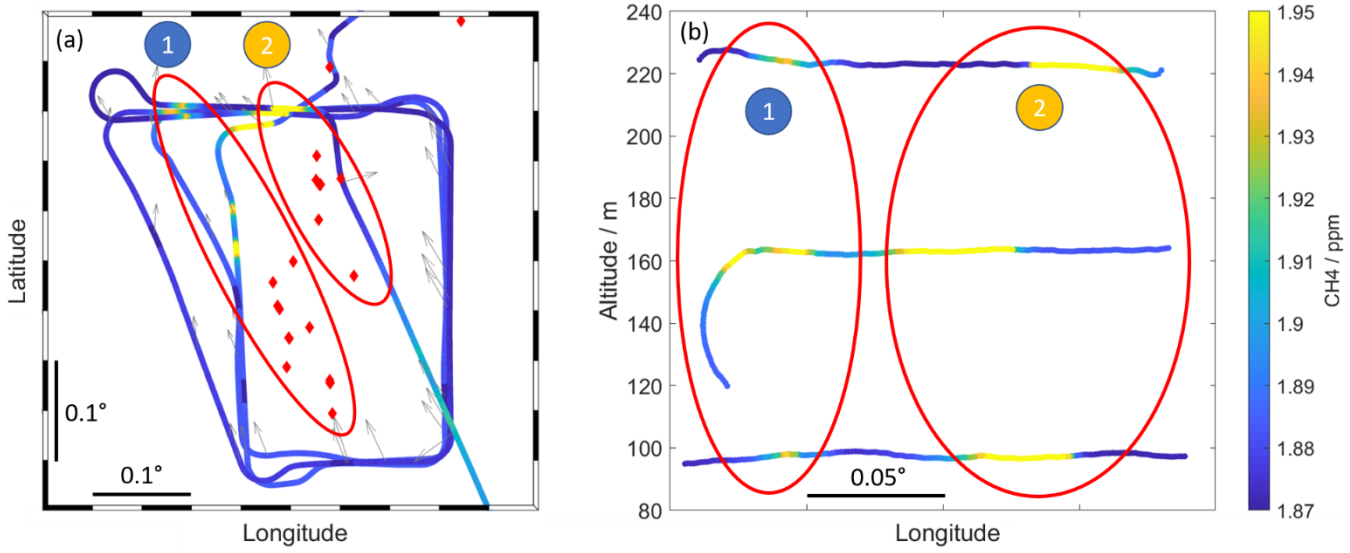

Figure 2: (a) Box pattern flown around two groups of facilities at different altitudes with adjustments to capture the entire plume along the northern wall. Red diamonds show the locations of facilities and the arrows the wind direction. Red ovals show the groups of facilities for each observed plume. (b) Three transects of the northern wall at different altitudes with plumes 1 and 2 marked. Latitude and longitude values are not specified to protect the anonymity of the operators.

2.3 Bottom up-emission inventory data

Methane and carbon dioxide emission data are available from global gridded bottom-up emission inventories like the Emissions Database for Global Atmospheric Research (EDGAR) from the European Commission JRC (2024), the Global Fossil Emissions Inventory v2 (GFEI) from Scarpelli et al. (2022) and the Copernicus Atmospheric Modeling Services Global anthropogenic emissions (CAMS-GLOB-ANT) (Granier et al., 2019; Soulie et al., 2023). In the EDGAR and CAMS inventories, the emissions are calculated using activity data, for O&G typically the amount of oil or gas produced, and an emission factor to derive regionally distributed emissions (European Comission JRC, 2024). The emissions are subject to uncertainties because the regional and temporal variation of emissions is often not accounted for in the calculation. The GFEI uses the countries' total emissions reported to UNFCCC and distributes them geographically according to activity data or other proxies like population density. Angola's last report of emissions to UNFCCC was in 2005 with a total CH_4 emission of 960 kt y^{-1} of which 487 kt y^{-1} are supposed to originate from the energy industry with the rest attributed to agriculture and the waste sector (UNFCCC, 2023). Scarpelli et al. (2020) scaled these emissions to 2019, the year of their inventory emissions. We used EDGAR v8.0, CAMS-GLOB-ANT v6.1, both for the year 2022, and GFEI v2 data for the year 2019. All three inventorial emissions are available on a global 0.1° x 0.1° grid.

The geographical distribution of the inventorial CH_4 emissions, along with the locations of facilities provided by the operators in Angola (black dots), is displayed in Figure 3. The red lines denote the border towards Congo and Democratic Republic of

https://doi.org/10.5194/egusphere-2025-635
Preprint. Discussion started: 21 February 2025

Congo. The geographical distribution in EDGAR matches well with the locations of the facilities. Only very few facilities are not covered by emissions and few emitting regions do not include a facility. In the GFEI distribution, however, there are many pixels containing emissions that do not contain a facility. The emissions are more evenly distributed and do not always show hotspot pixels at facility locations. The CAMS-GLOB-ANT emission dataset shows only very few and small emission spots offshore, which are collocated with facilities. The CO_2 emission maps are shown in the Appendix Figure B1.

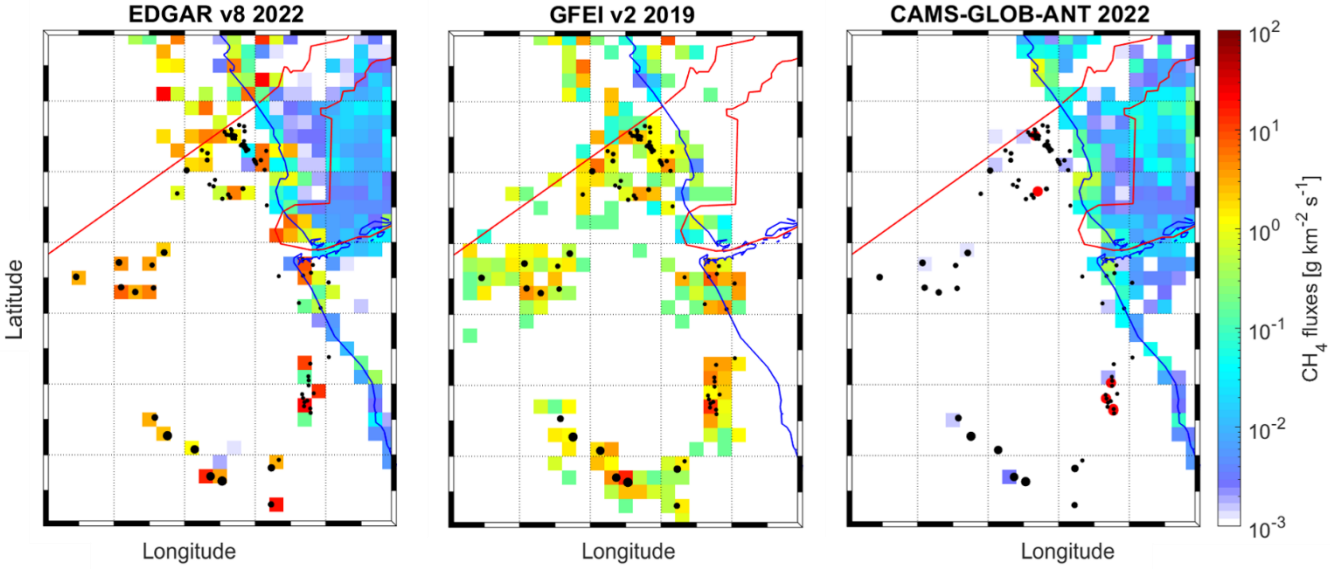

Figure 3: Maps of Angolan offshore region with CH_4 emission from the three gridded emission inventories. The black dots denote the Angolan facilities and their size is relative to their oil production in 2021 as reported by the operators. The red lines show the borders to Republic of Congo and the Democratic Republic of the Congo. The red circles in the right figure show MARS methane emission detection locations (see Section 2.5). Latitude and longitude values are not specified to protect the anonymity of the operators.

2.4 Operator reported data

Currently, there are seven companies operating offshore oil facilities in Angola. In the following they are treated anonymously and are called Operator A to G. The Angolan offshore sector is organized in so-called blocks. This is the administrative unit used by the Angolan Agency of Petroleum and Gas (ANPG, Agência Nacional de Petróleo, Gás e Biocombustíveis). ANPG is the administrative agency responsible for reporting on the O&G sector to the Angolan Ministry of Mineral Resources, Oil and Gas (MIREMPET, Ministério dos Recursos Minerais, Petróleo e Gás Angola), which actively supported the present study and facilitated the communication with the operators. Both from ANPG and the operators we received detailed data on the O&G exploitation and environmental impacts in Angola.

https://doi.org/10.5194/egusphere-2025-635
Preprint. Discussion started: 21 February 2025

The operators were informed about the upcoming measurement campaign to ensure safe flight operations, particularly regarding helicopter traffic and situational awareness. However, the specific timing of the measurements was not disclosed to the operators to prevent any potential operational changes that could bias the results.

Before the start of the measurement campaign we received the following facility information from the operators for 2021: name of facility, type of facility, block, year of commissioning, location, corresponding oil field, amount of oil produced, amount of gas produced, flare height, CH_4 emission, CO_2 emission. Following the campaign, we also received daily operational status and daily or monthly sums of: Oil produced, gas produced, gas burned, gas injected, fuel gas, lift gas, and gas exported to Angola LNG project (ALNG), emissions of CO_2 from fuel and flaring gas, CH_4 from flaring and fugitive for 2022. Where 2022 production or emission data were not provided, the annual data from 2021 or conversion ratios from other operators have been used to estimate emissions based on the amount of oil and gas produced.

The CH_4 and CO_2 emissions that we compare with our mass balance estimate were reported directly or calculated from reported proxies to ensure the best temporal resolution possible for each operator. Operator B and G directly reported all requested parameters in daily resolution. Operator E reported daily data of O&G production and fuel and flaring gas amounts and monthly emission data. Then daily emission data was calculated from the fuel and flaring gas amounts using the emission ratios per amount of fuel or flaring gas from operator B. The ratios used were 67.5 t CO_2 /mmscf (million standard cubic feet) for fuel gas and 74.5 t CO_2 /mmscf for flaring gas and 0.41 t CH_4 /mmscf from flaring. The calculated daily emission data fits with the reported monthly emissions within 1% for CO_2 and 20% for CH_4. Operator D reported monthly fuel and flaring gas amounts. This was transferred into emission data using the same ratios from operator B and downscaled to daily data assuming temporally constant emissions. Operators A, C, and F did not report facility-level emissions for 2022 but did provide annual emissions data for 2021. We downscaled these 2021 facility values under the assumption of temporally constant emissions, which aligns well with the operator totals reported for September 2022.

2.5 Satellite data

The IMEO data portal provides data from several satellite products to detect very large methane emissions around the world (UNEP, 2024). In total, it lists seven detected methane plumes from five facilities in the offshore region of Angola between November 2022 and August 2024. The locations are shown in Figure 3. All detected plume locations except for one detection collocate with Angolan offshore installation groups. The operator in the region of the unallocated detection has indicated that there are development projects in this region and the emission could result from a drilling ship or exploratory facility. Facility group F1* has three detections including the strongest emission plume of 9.19 ± 4.60 t h^{-1}.

https://doi.org/10.5194/egusphere-2025-635
Preprint. Discussion started: 21 February 2025

3 Results and discussion

3.1 Facility-scale emissions

In Figure 4 we display the methane emissions observed for individual facilities and groups of facilities. We were able to determine fluxes from 30 individual facilities and 10 facility groups (marked with an asterisk). Measurements have been repeated on different days and each observation is depicted separately. For 9 cases, the methane flux is set to zero, because it is below our theoretically lowest detectable flux. The lowest detectable flux is calculated for each mass balance individually and is between 0.8 and 10.3 kg h^{-1} CH_4. The total uncertainty includes the statistical uncertainty from trace gas and wind observations, the uncertainty of the background, and the uncertainty of the plume height. For the latter, the number of transects flown through the plume is crucial. The mean total 1-sigma uncertainty for all mass balances is 29% mainly resulting from the uncertainty of the plume height, which contributes 77% to the total uncertainty. The uncertainty of small fluxes is dominated by the statistical uncertainty, while larger fluxes depend much more on the uncertainty of the plume height. The uncertainty and lowest detectable flux calculation are described in detail in Appendix A.

For most facilities, the observed CH_4 emissions are similar on different days and show little temporal variability (Figure 4). As an exception, on one day we captured a high-emission event of 10.4 t h^{-1} from platform D3. On another day, though, the emissions from this facility were only 0.02 t h^{-1}. The operator commented that nothing special happened on this platform during the time of the campaign. The plume is clearly attributable to D3 and was measured several times up to a distance of 75 km from the facility. The relevance of such an event heavily depends on its duration. Since we do not know about the duration in our case, we weighed both events equally, which results in mean emissions of the facility with a high total uncertainty of 100% (5.2 ± 5.2 t h^{-1}). This approach integrates high-emission events into the average emissions of the entire Angolan offshore O&G sector. By capturing a substantial ensemble of measurements (87 mass balances across 57 facilities over 2.5 weeks) the intermittent nature of these high-emission events is accounted for in the overall assessment.

Another facility group with high methane emissions is from operator F with three measurements between 3.5 and 4.1 t h^{-1} on the first two measurement days (four days apart) and one of 1.3 t h^{-1} during the last measurement two days afterwards (F5*). This shows that the high emissions were not consistent, but occurred for at least four days. Operator F also reported normal operations for all their facilities during the measurement flights. Both high-emission event facilities (D3 and F5*) are shallow water platforms built in the 1980s (see Section 3.3). Unfortunately, we do not have production or emission data with daily resolution from operators D and F. This might have provided more insight into the causes of the variability in emissions, and the frequency or duration of these events.

The status of operations on each facility during the measurements was inquired from the operators directly. We received information from all operators except for operator C. Measurements during special operations are marked by a black outline in Figure 4. Special operations encompass anything that falls outside of standard procedures, e.g. shutdown, maintenance, offloading of oil to a tanker, gas export offline, and seawater system bond strand piping repair (injection offline). There were 7 cases of special operations reported for the total of 87 measurements. They do not coincide with high emissions, but rather

https://doi.org/10.5194/egusphere-2025-635
Preprint. Discussion started: 21 February 2025

show low emissions and one medium emission strength of 0.3 t h^{-1} at facility B3 during offloading. It should be noted, however, that we visited only briefly for each measurement. The reported special operations may have taken place during a different time of day, causing the measurement to miss associated emission changes. Notably, during the high-emission events the operators reported normal operations. This probably means that they were not aware of their high emissions. This is the type of emission that is hardest to mitigate because of the missing awareness of the emission.

In general, higher emissions often originate from groups of older platforms in the shallow water regions (operators C, D, and F). One of these groups includes 28 facilities with all kinds of platforms like living, production, flaring and well jackets. Deep and ultra-deep water facilities (operators B, E, G) tend to emit less with emissions ranging between the detection limit and 0.3 t h^{-1}. This is further examined in Section 3.3.

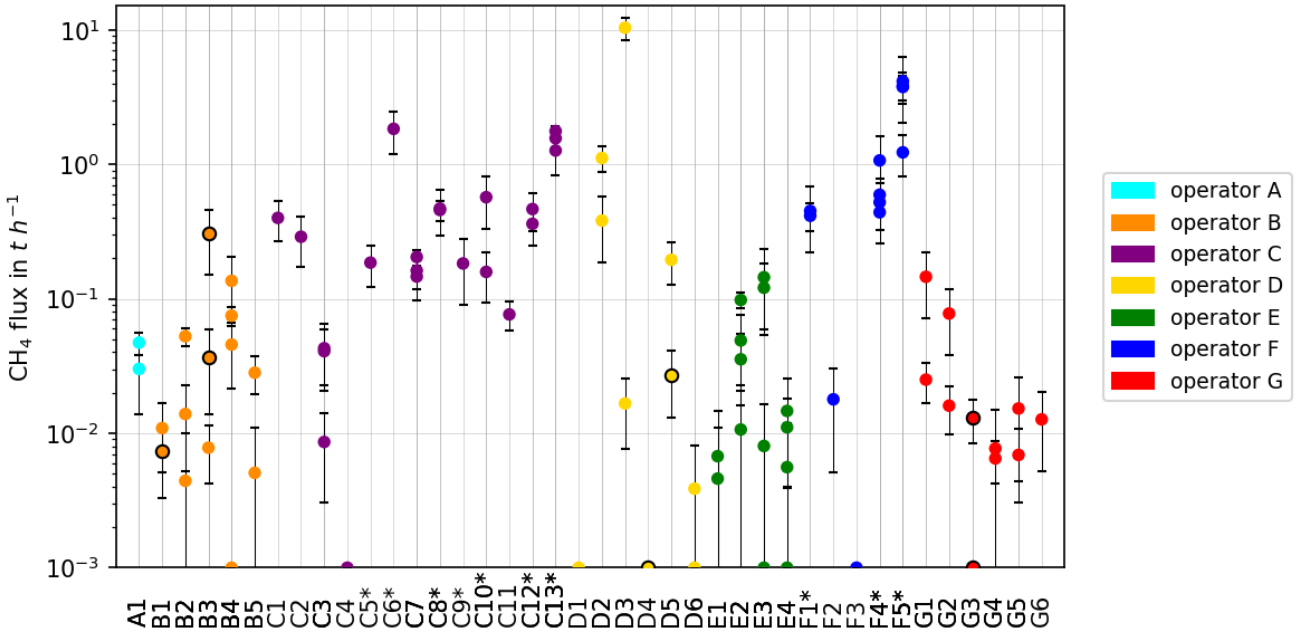

Figure 4: CH_4 emissions determined from mass balance flights during MTGA for 30 individual facilities and 10 groups of facilities in Angola. The groups are marked with *. Markers at 10^{-3} t h^{-1} are below the theoretically lowest detectable flux and counted as zero. Emission estimates, where operators reported special operations, are marked by a black outline.

3.2 Parameters impacting CH_4 emissions

Based on observations of other trace gases and data provided by the operators, we aim to identify the causes of the observed CH_4 emissions. Figure 5a compares the CH_4 fluxes with the measurement-based CO_2 fluxes at various facilities. High CO_2 emissions with low CH_4 levels suggest that the emissions likely result from combustion processes, such as flaring or stationary combustion in engines. Conversely, large CH_4 emissions with low CO_2 levels point to leaks or venting as the source. In Angola,

https://doi.org/10.5194/egusphere-2025-635
Preprint. Discussion started: 21 February 2025

the major CH_4 emission events seem to originate from leaks or venting, as these plumes show minimal CO_2. Facilities with high CO_2 emissions tend to release little CH_4, indicating efficient flaring or turbine operations. During our campaign, we conducted targeted samples of seven flaring plumes in Angola, with detailed analyses of these flares to be published in a follow-up study. Figure 5b highlights CH_4 emissions in relation to the commissioning year of each facility, showing that the highest-emitting facilities tend to be those commissioned before 2000. These older facilities, located in shallow waters closer to the coast, are operated by companies C, D, and F. Figures 5c and 5d compare the measured CH_4 emissions to O&G production data from September 2022 or, if unavailable, the average production in 2021. High-production facilities, operated by A, B, E, and G, generally exhibit low emissions, while high-emitting facilities, mostly run by C, D, and F, show lower production volumes. This is particularly evident in gas production, due to the division of Angolan offshore facilities into those connected to the LNG plant and those that are not. The older facilities (C, D, and F) are not connected to the gas pipeline feeding the LNG plant. Instead, associated gas is reinjected, captured, or flared. Since this gas lacks economic value, potential leaks may not be closely monitored.

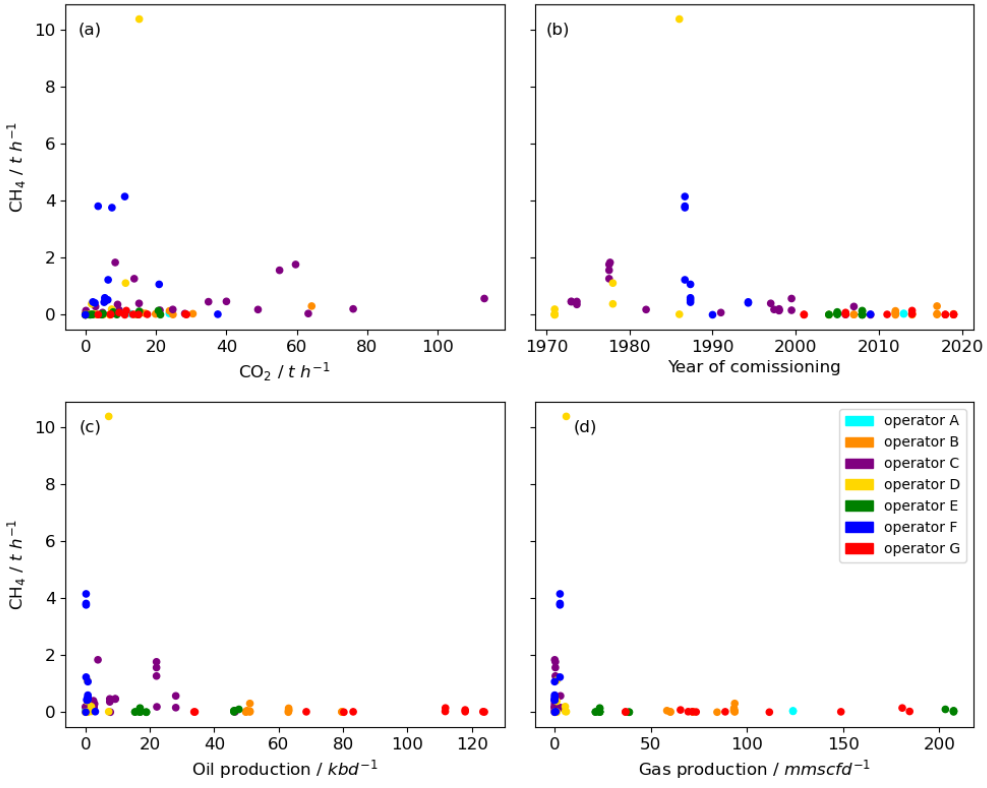

Figure 5: Observed CH_4 emissions of the Angolan facilities in relation to (a) CO_2 emissions, (b) year of commissioning of the facility (average for groups), (c) oil production in 2021/2022 in kbd^{-1} (kilo barrel per day), and (d) gas production in 2021/2022 in $mmscfd^{-1}$ (million standard cubic feet per day).

https://doi.org/10.5194/egusphere-2025-635
Preprint. Discussion started: 21 February 2025

Figure 6 shows the relations of CH_4 emissions to other trace gases measured on the Falcon aircraft during MTGA (CO, C_2H_6, SO_2, and NO_y). Carbon monoxide (CO) is an indicator for incomplete combustion processes and, thus, maybe malfunctioning flares or turbines. Some of the older facilities from operator C emit more than 200 kg h^{-1} of CO along with their high CO_2 emission (see Figure 5a). The high-emission event on facility D3 is also accompanied by elevated CO emissions of 160 kg h^{-1}. High CH_4 emissions from operator F are not accompanied by emissions of CO. Figure 6b depicts the strong correlation between CH_4 and C_2H_6 emissions. This results from the common source of CH_4 and C_2H_6 as components of the associated natural gas. The average molar C2/C1 emission ratio is 15 ± 6 %. It is within the composition range of associated gas of 10-25 % (Xiao et al., 2008). Operator reports on the molar C2/C1 ratio of several facilities range from 5% to 20%. This matches with our observations. Figure 6c shows elevated SO_2 emissions from two onshore facilities of 37 kg h^{-1} (A1) and 49 kg h^{-1} (D6) without accompanying CH_4 or CO_2 emissions. The high-emission event from facility D3 is also accompanied by 20 kg h^{-1} of SO_2. This facility's gas is reported to contain H_2S, which after combustion turns into SO_2. Figure 6d displays the NO_y emissions observed from the aircraft, with NO_y serving as an additional tracer for combustion processes. Notably, NO_y emissions show no correlation with CH_4 emissions, and for facility F5, varying levels of NO_y emissions were detected even when CH_4 emissions remained at 4 t h^{-1} across different days. This lack of correlation suggests that the CH_4 emissions are not from flaring but are likely due to venting or leakage.

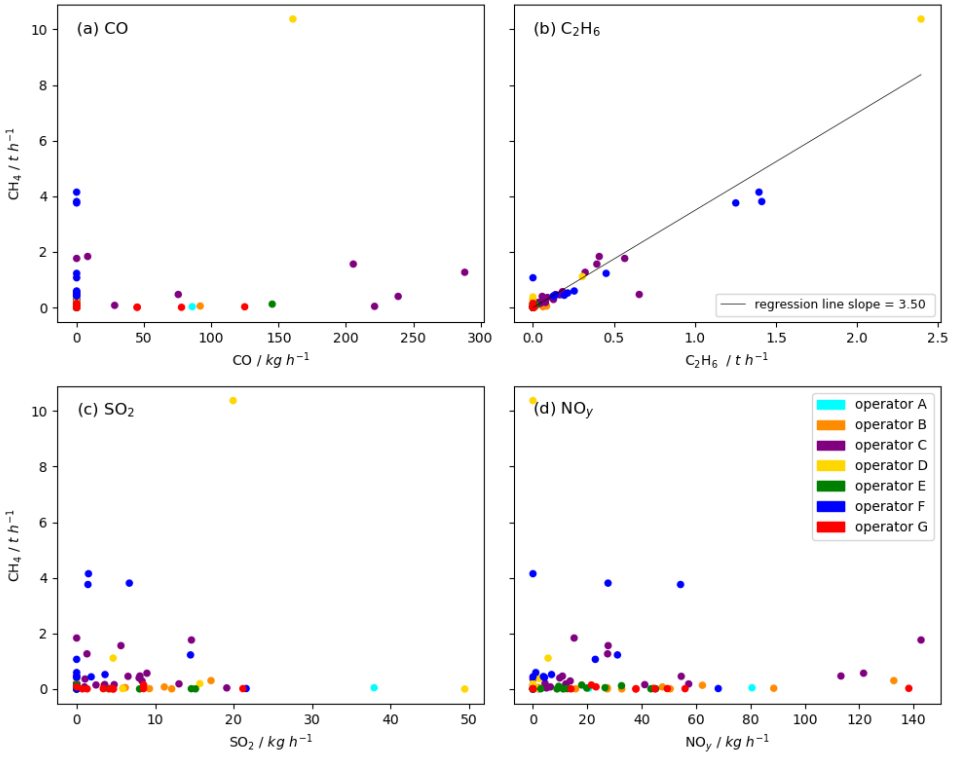

Figure 6: Relationship between measured CH_4 and other trace gas emissions (CO, C_2H_6, SO_2, and NO_y) from individual facilities/groups of facilities for single measurements.

https://doi.org/10.5194/egusphere-2025-635
Preprint. Discussion started: 21 February 2025

This analysis of our emission estimates, informed by operator data and observations of additional trace gases, allows for a more nuanced interpretation of our results. We find no correlation between CH_4 and CO_2 emissions, suggesting that they originate from different processes or sources on these facilities. CH_4 emissions are largely driven by older, low-production, shallow-water facilities, whereas high-production facilities, primarily newer FPSOs in deep and ultradeep water, exhibit relatively low CH_4 emissions despite their high output levels. This leads us to propose a shift away from production data as a proxy for methane emissions; instead, age, maintenance condition, or facility type (shallow- vs. deep-water) may serve as more reliable indicators of methane emission strengths.

3.3 Comparison of observed emissions with operator reporting

The aircraft-based observations of average methane emissions from individual facilities or facility groups in Angola are shown in comparison with operator-reported emissions in Figure 7. Here we compare average observed emissions for each facility, calculated from the individual observations displayed in Figure 4. A broader comparison of total Angolan emissions with gridded inventory data and operator reporting is available in Section 3.6. We avoid comparing observations with gridded inventories at the facility level due to the limited number of samples per grid box, the significant uncertainties in attribution within global inventories, and the differing timescales between the two methods.

The operator data is described in detail in Section 2.4. For operators B, E, and G, the values are based on daily reports in September 2022. Operator D reported monthly fuel and flaring gas amounts for 2022, which were converted into emissions data. Operators A, C, and F did not report facility-level emissions for 2022 but provided annual data for 2021, which we downscaled. Only one operator directly reported fugitive emissions of CH_4. All other operators only report CH_4 emissions derived from flaring. Reported CO_2 emissions result from flaring and fuel gas combustion.

The CH_4 emissions reported by operators (Figure 7a) are generally lower than the observed emissions, with maximum reported emissions at 1.5 t h^{-1} for facility C3, where no significant emissions were measured. In contrast, for top-emitting facility D3 only 0.1 t h^{-1} are reported by the operator as flaring emissions while fugitive emissions are not accounted for. Generally, emissions from older facilities (operators C, D, and F), from which we captured high-emission events, tend to be underestimated by operators, while emissions from newer, high-production facilities (operators A, B, E, and G) are often overestimated.

https://doi.org/10.5194/egusphere-2025-635
Preprint. Discussion started: 21 February 2025

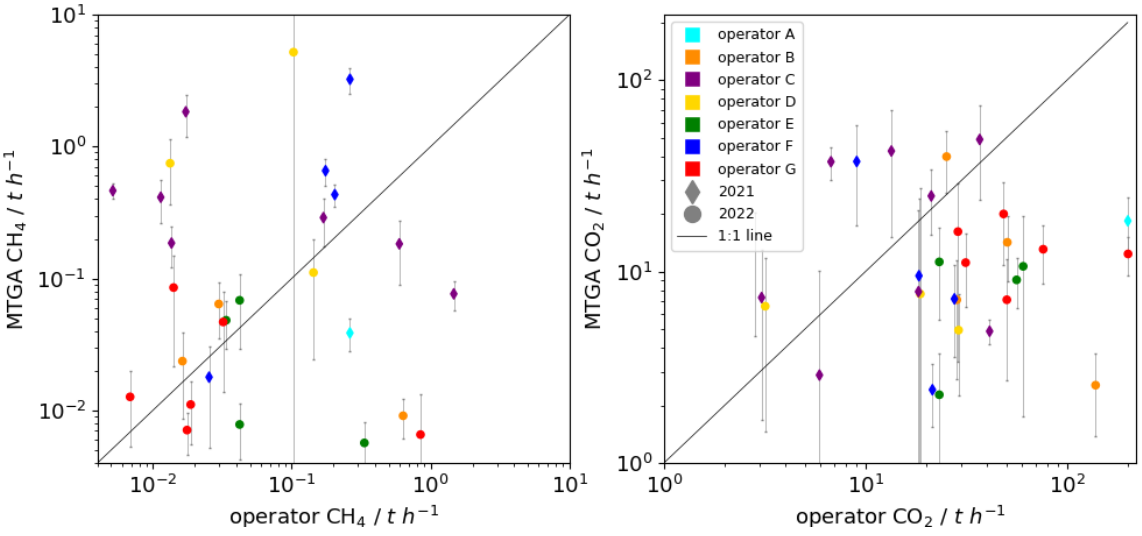

Figure 7: Observed average CH_4 and CO_2 emissions of the Angolan offshore facilities or groups of facilities compared to operator data consisting of daily or monthly reports for September 2022, or if not available downscaled annual data for 2021.

A comparison of observed CO_2 emissions with operator reports (Figure 7b) shows generally higher reported emissions than observed. CO_2 emissions result from the combustion of natural gas in gas turbines or flares, with gas use closely monitored and reported. However, CO_2 emissions reported by newer facilities (operators A, B, and G) are up to ten times higher than observed. This discrepancy could stem from the different timescales of our sampling and operator reports, especially since intermittent flaring often occurs during special operations. Notably, we did not observe any high CO_2 emission events from newer facilities. The observed atmospheric CO_2 enhancements for fluxes below 40 t h^{-1} were often around the instrument uncertainty of 0.34 ppm. They were clearly distinguishable from the background fluctuations, though, and could be used for emission estimation.

Our measurements capture random snapshots of emissions, which are inherently variable across facilities, whereas operator reports reflect time-averaged emissions. These differences are expected at the facility level. However, they highlight two potential areas for improvements: collecting larger ensembles of observations to smooth short-term emission fluctuations, or enhancing the time resolution of operator reporting to enable more direct comparability at the facility level.

https://doi.org/10.5194/egusphere-2025-635
Preprint. Discussion started: 21 February 2025

3.4 Comparison with satellite data

The IMEO data platform provides a valuable resource for tracking methane emissions by listing and quantifying plumes observed via satellite (see Section 2.5). For the Angolan offshore region, seven methane plumes have been quantified from five distinct locations between November 2022 and February 2024 (Figure 8). All except one detection were allocated with groups of facilities in the shallow-water region of the Angolan offshore exploitation. Emission estimates from groups C15* and F5* agree within uncertainties. Facility group F4* showed lower emissions during aircraft observations than from the satellite detection. Group F1* had three satellite detections. One of them has the highest satellite detected value with 9.19 ± 4.60 t h^{-1}. This is in the range of the high-emission event detected by aircraft from facility D3. Here, the satellite probably captured high-emission events from one of the facilities in group F1*. This event is in the range of the high-emission event detected by aircraft from facility D3. The mean airborne emission observations of F1*, however, were as low as 0.43 ± 0.22 t h^{-1}.

While satellite observations are critical for identifying major emission sources, they cannot capture every emission event due to limited temporal and spatial resolution. Additionally, the current imaging satellites have detection limits around 1 t h^{-1}. This underscores the need for complementary ground-based or aircraft-based measurement campaigns to verify operator-reported emissions and detect fugitive emissions that may go unnoticed. Regular monitoring, particularly of high-risk facilities such as older or poorly maintained infrastructure, can help ensure accurate reporting and provide actionable data for mitigation.

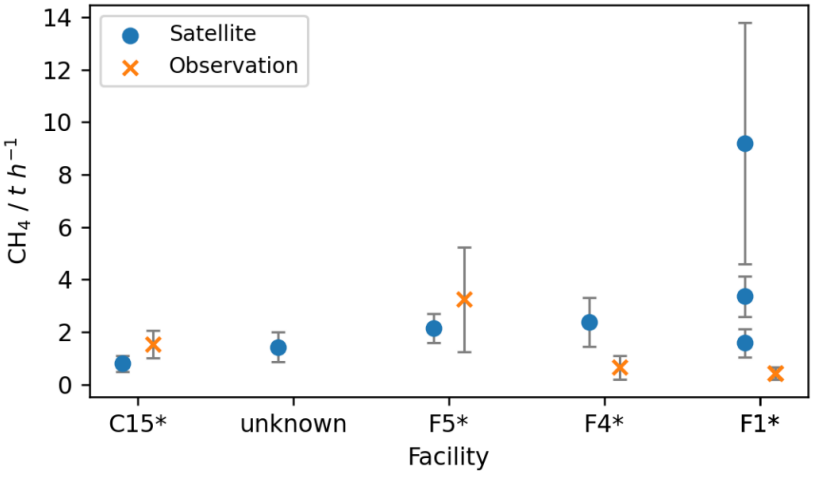

Figure 8: Comparison of mean aircraft mass balance emission estimates with IMEO satellite detections. The second detection could not be attributed to a facility. Facility F1* has three satellite detections.

https://doi.org/10.5194/egusphere-2025-635
Preprint. Discussion started: 21 February 2025

3.5 Comparison with other offshore production regions

A comparison of our CH_4 emission estimates from the Angolan offshore facilities with other airborne measurements from offshore regions in the world was carried out. Figure 9 shows a histogram of our estimated fluxes of individual and groups of facilities and the corresponding mean. The mean was calculated by dividing total observed emissions by the 57 facilities that were measured individually or in groups. The red lines are the average emission estimates of offshore facilities in the Norwegian Sea, Southern North Sea and the Northern Gulf of Mexico (Foulds et al., 2022; Gorchov Negron et al., 2023; Pühl et al., 2024). Average Angolan emissions per facility (0.30 t CH_4 h^{-1}) are smaller than the emissions in the Northern Gulf of Mexico (0.46 t h^{-1}). In both regions the focus is on oil production and facilities are partly old. Average facility emissions in the Norwegian Sea (0.03 t h^{-1}) and Southern North Sea (0.14 t h^{-1}) are lower. In these regions, facilities tend to be more modern and mostly produce gas, which explains the lower emissions. More detailed comparisons and discussions, including other studies and regions, are planned within the IMEO framework.

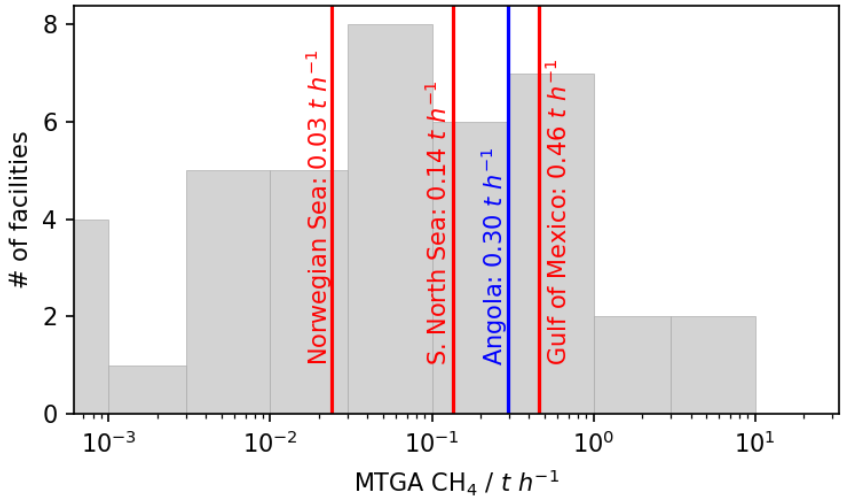

Figure 9: Histogram of our estimated mean CH_4 fluxes of individual facilities and groups of facilities off the coast of Angola. The average value is marked in blue and calculated using the total number of facilities in each group. For comparison, average CH_4 emission estimates for the Norwegian Sea, the Southern North Sea and the Northern Gulf of Mexico are indicated in red (Pühl et al., 2024).

3.6 Total Angolan emissions and emission indices

The total Angolan offshore emissions of CH_4 and CO_2 derived by airborne mass balance during MTGA is calculated as the sum of mean emissions from all facilities. This leads to total emissions of 16.9 ± 5.3 t CH_4 h^{-1} and 613 ± 105 t CO_2 h^{-1} including the high-emission events. The 10 t h^{-1} CH_4 emission event from platform D3 stands out, representing over half of Angola's total offshore emissions, highlighting the significance of such high-emission events. The frequency and duration of these

https://doi.org/10.5194/egusphere-2025-635
Preprint. Discussion started: 21 February 2025

events have a substantial impact on the country's overall emissions. The large ensemble of our measurements is deemed to capture the intermittent nature of high-emission events, incorporating them into the overall assessment.

Several gridded inventories also report offshore emissions for Angola (Figure 10). We summed the gridded inventories in the entire offshore region. The observed CH_4 emissions are only 20% and 22% of what is provided in the EDGAR v8.0 and GFEI v2 inventories, respectively. CAMS report very low emissions of only 1.4 t h^{-1}. The International Energy Agency's (IEA) Methane Tracker provides emissions data at the country level while distinguishing between various sectors. In Angola, total energy sector emissions are reported at 98 t h^{-1}, with 86 t h^{-1} attributed to the offshore sector. These emissions are divided into fugitives (19%), venting (74%), and flaring (7%). The IEA's estimates align with the ranges reported by EDGAR and GFEI. The overestimation of inventory CH_4 emissions in Angola is indicative of a broader trend in which bottom-up inventories tend to overestimate emissions from offshore O&G production (Shen et al., 2023). In Angola, the overestimation of emission factors for newer Floating Production Storage and Offloading units (FPSOs) in inventories may contribute to discrepancies. These advanced facilities typically employ better technology and maintenance, resulting in emissions that are lower than those predicted by standard emission factors. Reassessing these factors could enhance inventory accuracy. Furthermore, operator-reported emission rates for 2021/2022 and the Second National Communication (SNC) of Angola to UNFCCC with the last emission report for 2015 (Republic of Angola, 2021) are nearly three times lower than observation-based estimates. Most operators focus on reporting methane emissions related to flaring and combustion, largely neglecting fugitive emissions. While we recognize the challenges in quantifying fugitive emissions without direct measurements, the gap between our observations and reported figures highlights the urgent need for regular monitoring at each facility to identify and mitigate fugitive emissions.

The observed CO_2 emissions of 613 ± 134 t h^{-1} are close to the EDGAR v8.0 inventory emission of 690 t h^{-1}. CAMS v6.1 emissions of 1412 t CO_2 h^{-1} and the operator reported emissions of 1389 t h^{-1} for 2022 are twice as high as the observed or EDGAR emissions. The offshore CO_2 emissions originate from flaring or combustion. Operators can typically calculate their combustion emissions with precision, as the volume of burned gas is closely monitored and required to be reported. However, our flights may have missed a portion of CO_2 emissions when they did not reach the upper half of the boundary layer, where hot flaring exhaust initially rises due to buoyancy, only dispersing at greater distances from the source. This effect, shown in Figure A1, may partly explain the discrepancy between measured and reported CO_2 emissions, along with the challenges of aligning snapshot observations with emissions that vary over time due to operational shifts, maintenance, and other factors. Although we used a large set of measurements to capture a comprehensive picture, further sampling is necessary to better capture the temporal variability of the emissions. Comparing O&G production data from September 2022 with 2021 data indicated no significant differences, suggesting that our measurement period reflects typical operations.

https://doi.org/10.5194/egusphere-2025-635
Preprint. Discussion started: 21 February 2025

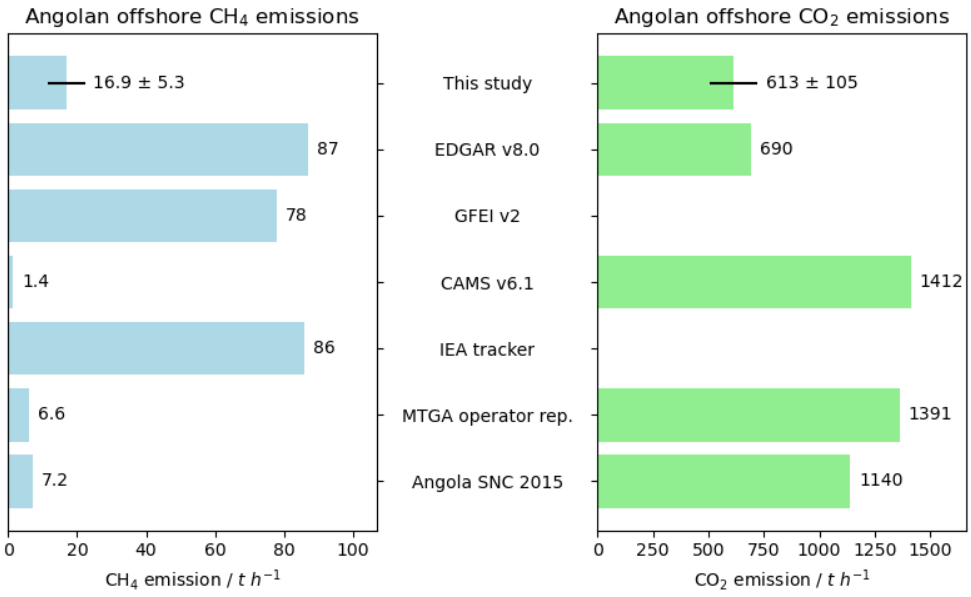

Figure 10: Total emissions of CH_4 and CO_2 for the Angolan offshore sector from observations, inventories, and reports. The International Energy Administration (IEA) methane tracker data was downloaded from their data portal (IEA, 2024). The Angola Second National Communication (SNC) to UNFCCC emissions are taken from the last emission report for 2015 (Republic of Angola, 2021).

Finally, we calculated the carbon and methane emission intensity of Angolan oil and gas from the total observed GHG emissions and total O&G production in September 2022. For the carbon intensity calculation, CH_4 emissions are transformed into CO_2eq using a global warming potential for 100 years (GWP100) for CH_4 of 29.8 (IPCC (2021)). The combined CH_4 and CO_2 Angolan offshore emissions are 28.5 ± 18.0 kt CO_2eq d^{-1}. The Angolan mean offshore production of oil and gas in September 2022 was reported to ANPG as 1099 kbd^{-1} produced and 600 $mmscfd^{-1}$ of gas exported to the LNG terminal, respectively. This puts the carbon intensity of Angolan offshore oil and gas at 3.6 ± 0.9 g CO_2eq MJ^{-1} for September 2022. The carbon intensity resulting from EDGAR emission estimates would be 8.2 g CO_2eq MJ^{-1}. Masnadi et al. (2018) estimated a carbon intensity for Angola of around 7.5 [6.6-14.1] g CO_2eq MJ^{-1} for 2015 which is in line with EDGAR estimates, but more than twice as high as our measured carbon intensity.

The methane emission intensity divides total volumes of CH_4 emissions from both oil and natural gas value chains of operated assets by the total volumes of marketed natural gas. To convert the 600 $mmscfd^{-1}$ of produced gas to a mass flux, we use the mean reported mole fraction of 78% of methane in the exported natural gas or the equivalent mean molar mass of 22 g/mol for Angolan natural gas. The observed methane intensity for September 2022 is then calculated to be 2.6%. Considering that Angola mainly produces oil with natural gas merely being a by-product we expect this high methane intensity. It is also caused by the high fraction of produced gas that is reinjected (53%) instead of exported. Shen et al. (2023) calculated the Angolan methane intensity to around 20% from methane emissions of 910 Gg a^{-1}, which corresponds to 103 t h^{-1}, and International Energy Agency gas production values for 2019.

https://doi.org/10.5194/egusphere-2025-635
Preprint. Discussion started: 21 February 2025

4 Summary

The dataset collected during the METHANE-To-Go Africa campaign is uniquely comprehensive, offering detailed measurements of CH_4 emissions from offshore O&G production along the West African coast, particularly Angola. Using an aircraft-based mass balance method, this analysis quantified emissions from all offshore facilities in Angola, with a focus on 30 individual facilities and 10 facility groups. Benefiting from stable wind conditions during flights, the mean 1-sigma uncertainty for methane emissions is 29%. Additional trace gas measurements, including CO_2, CO, C_2H_6, SO_2, NO_y, and aerosol particles, provided further insights into sources of CH_4 emissions.

Our results show mainly consistent emission estimates across different days for most facilities, with minimal temporal variation. However, two facilities exhibited high-emission events of 10 and 4 t h^{-1} on specific days, emphasizing the importance of capturing such events for total emissions estimates. Operator reports indicate that normal operations were in place during our observation periods, suggesting that these high emissions were unknown to them and likely due to leaks. Although satellite detections also reveal high-emission events from other facilities, the limited number of detections—just seven over three years—makes it difficult to assess the duration or frequency of these events. Enhanced operator awareness and more detailed reporting are essential to gain a clearer understanding of their impact.

Our findings suggest that significant CH_4 emissions in Angola stem from leakages or venting, as low CO_2 concentrations in plumes indicate limited flaring. Combustion processes in flares and turbines appear efficient, with high CO_2 emissions not being accompanied by elevated CH_4. Our observations indicate that high CH_4 emissions primarily occur at older, low-producing facilities, while newer, high-producing FPSOs in deep and ultradeep water emit comparatively little methane. Production volume is again shown to be a poor estimator of emissions. To improve bottom-up emission estimates, we recommend considering facility age or maintenance status as factors that introduce additional risk for methane emissions, rather than purely relying on production volume as a proxy. Nevertheless, given the significant variability in asset design and operation, measurements remain crucial. Regular measurements by e.g. operators should prioritize high-risk facilities, such as older ones.

Satellite detections of methane plumes offshore of Angola remain sparse, with seven observed plumes showing emission levels similar to our observations, including the enhanced emissions of the high-emission events that we observed at other facilities during the airborne campaign. The average observed airborne CH_4 emission of Angolan offshore facilities was calculated at 0.30 t h^{-1}, lower than that of the Gulf of Mexico (0.46 t h^{-1}) but higher than the Norwegian Sea (0.03 t h^{-1}) and Southern North Sea (0.14 t h^{-1}).

Total emissions from Angolan offshore facilities were measured at 16.9 ± 5.3 t CH_4 h^{-1} during MTGA, representing 20% of EDGAR and 22% of GFEI inventory levels. Operator data for 2021 and 2022 underestimate CH_4 emissions by two-thirds

https://doi.org/10.5194/egusphere-2025-635
Preprint. Discussion started: 21 February 2025

relative to observations, with most operators only reporting flaring-related emissions and omitting fugitive emissions. We acknowledge the challenge in estimating fugitive emissions without measurements. However, this discrepancy underscores the importance of regular monitoring to detect and mitigate these emissions. Total observed CO_2 emissions are 613 ± 105 t h^{-1}, which is close to the EDGAR v8.0 inventory emission of 690 t h^{-1}, but less than half of the CAMS v6.1 emissions of 1412 t CO_2 h^{-1} and the operator reported emissions of 1389 t h^{-1} for 2022. The significant differences between measured and reported emissions likely result from overestimated emission factors for newer FPSOs, underreporting of fugitive emissions, and the challenges of aligning snapshot observations with intermittent emission events.

The observed carbon intensity of Angolan oil and gas stands at 3.6 ± 0.9 g CO_2eq MJ^{-1} for September 2022, less than half of previous estimates. The observed methane intensity of Angolan gas is 2.6%, expectedly high for a country where gas is mainly a by-product of oil production.

This study was made possible through strong collaboration with ANPG, MIREMPET, and local O&G operators, whose support was invaluable. Our findings were presented to local partners in Luanda, Angola, in October 2022, where operators received feedback on their emissions. They expressed significant interest in a follow-up campaign, and ANPG is planning to implement more comprehensive reporting requirements and mandate operators to reduce CH_4 emissions in the future.

By providing a uniquely detailed dataset on CH_4 emissions from Angola's offshore O&G industry, this study substantially enhances our understanding of emission sources and patterns in this oil and gas-producing region.

https://doi.org/10.5194/egusphere-2025-635
Preprint. Discussion started: 21 February 2025

Appendix A: Mass balance method uncertainties

The uncertainty of our emissions calculated with the mass balance method is combined from the statistical uncertainty, originating from the uncertainty in the measured parameters, and the systematic uncertainty, caused by the assumptions made for the method. The statistical uncertainty is calculated based on the measurement uncertainties, which are propagated through the mass balance equations using Gaussian error propagation. The uncertainties of the measured parameters are shown in Table A1. The uncertainty of the background concentration c_0 is calculated as the standard deviation of the background interval. Here, we list the equations and respective uncertainty calculation of the parameters, which are marked with u_x:

Concentration enhancement: $\Delta c_i = c_i - c_0 \quad \Rightarrow \quad u_{\Delta c_i} = \sqrt{{u_{c_i}}^2 + {u_{c_0}}^2}$

Flux for each timestep i: $F_i = \frac{\Delta c_i \, v_i \, p_i \, dx_i \, M \, D_t}{R \, T_i} \quad \Rightarrow \quad u_{F_i} = F_i \sqrt{\left(\frac{u_{\Delta c_i}}{\Delta c_i}\right)^2 + \left(\frac{u_{v_i}}{v_i}\right)^2 + \left(\frac{u_{p_i}}{p_i}\right)^2 + \left(\frac{u_{dx_i}}{dx_i}\right)^2 + \left(\frac{u_{D_t}}{D_t}\right)^2 + \left(-\frac{u_{T_i}}{T_i}\right)^2}$

Here M is the molar mass of the gas and R is the universal gas constant.

Flux for each transect t and statistical uncertainty: $F_t = \sum_i F_i \quad \Rightarrow \quad u_{F_{stat}} = \sqrt{\sum_i {u_{F_i}}^2}$

Table A1: Measurement parameters with instrument and measurement uncertainty during the MTGA campaign.

Symbol	Parameter	Instrument	Measurement uncertainty (1σ, 1s)
c_i CH_4	concentration of CH_4	Aerodyne QCLS	1.55 ppb (Kostinek et al., 2019)
c_i CH_4	concentration of CH_4	Picarro G2401-m	1.25 ppb (after Klausner, 2020)
c_i CO_2	concentration of CO_2	Picarro G2401-m	0.34 ppm (after Klausner, 2020)
c_i C_2H_6	concentration of C_2H_6	Aerodyne QCLS	0.24 ppb (Kostinek et al., 2019)
v	horizontal wind speed (u and v direction)	Flow angle sensor	4 % (Giez et al., 2022)
p	pressure	Flow angle sensor	50 Pa (Bramberger et al., 2017)
x	horizontal distance	IGI GNSS/IMU: Compact FOG-I	0.02 m (AEROcontrol)
D	depth of each transect layer	IGI GNSS/IMU: Compact FOG-I	0.20 m (AEROcontrol)
T	temperature	PT100	0.5 K (Fimpel, 1991)

The systematic uncertainty for our mass balance approach mainly consists of the uncertainty of the background concentrations and the plume height uncertainty. We estimated the uncertainty of these two parameters for each transect individually. For the background value uncertainty, we calculated the flux using an average background concentration from an upwind flight track if an upwind flight track was available. The uncertainty was then defined as the difference between the flux using upwind background and the standard background from the edges of the plume. This was available for 16 of the total 99 mass balances.

https://doi.org/10.5194/egusphere-2025-635
Preprint. Discussion started: 21 February 2025

The average uncertainty due to the background was 10% of the total flux for these cases. Therefore, we added a background uncertainty of 10% to all mass balances without upwind data.

The plume height uncertainty relates to our assumption that every observed plume reaches from the ocean surface to the top of the PBL. We measured the plumes at distances between 4 and 15 km from the source, with most flight tracks between 5 and 10 km distance. This should allow the plume to be well mixed and reach uniform concentrations between the ocean surface and the PBLH. The cases where we have several transects at different altitudes showed average concentrations in the middle of the PBL, but we never measured directly at ocean surface nor at PBLH level (see Section 2.2). We assumed that the plume depth toward the ocean surface is uncertain up to half the height of the lowest flight transect. Additionally, the plume height is uncertain between middle of the highest transect and the PBLH up to the PBLH. In this way we also accounted for the uncertainty in the determination of the PBLH. The method includes that the calculated flux becomes more uncertain the fewer transects we flew. The single transect mass balances were targeted to be flown in the middle of the boundary layer. An example of the uncertainties for single and multiple transect calculations is shown in Figure A1 for the racetrack flight pattern in Figure 1b. The transect at 250 m falls within the average CH_4 emission range, with the lower three transects below and the upper ones above the mean emissions. This behaviour was observed in several cases, but sometimes also with reversed profile. From this, we conclude that single transect mass balances are reliable when conducted in the middle of the planetary boundary layer (PBL). Below 150 meters, they should be used with caution, and above the middle level, emissions may be overestimated.

For each transect, the three individual uncertainties (statistical, background concentration, and plume height) are summed in quadrature to derive the emission uncertainty.

$$u_{F_t} = \sqrt{{u_{F_{stat}}}^2 + {u_{F_{bg}}}^2 + {u_{F_{ph}}}^2}$$

Finally, the total flux is calculated as sum of all transect fluxes: $F = \sum_t F_t \quad \Rightarrow \quad u_F = \sqrt{\sum_t {u_{F_t}}^2}$

In the case of having several measurements for a facility or group of facilities, we also calculate the mean emission per facility $\bar{F}$ from the single measurements. The uncertainty of the mean facility emissions $u_{\bar{F}}$ then is a combination of the uncertainties of the single measurements u_{F_i} and the standard deviation of the mean σ of these measurements with n being the number of single measurements: $u_{\bar{F}} = \sqrt{\left(\frac{1}{n}\sum_i u_{F_i}\right)^2 + \left(\frac{\sigma}{\sqrt{n}}\right)^2}$

https://doi.org/10.5194/egusphere-2025-635
Preprint. Discussion started: 21 February 2025

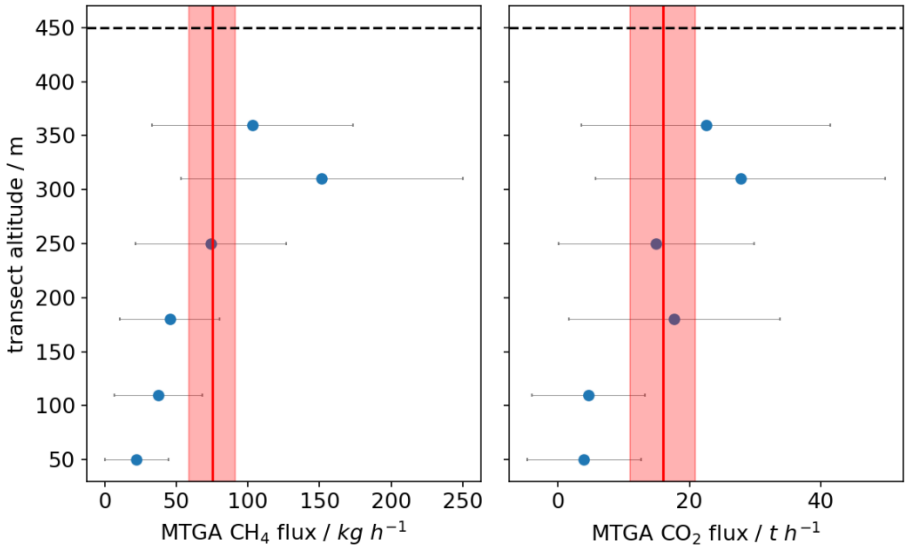

Figure A1: Mass balance estimates for each single transect including uncertainties as markers and the emission estimate using all transects and the layer method with uncertainty in red. The PBL was at 450 m. Transects in the middle of the PBL show good agreement with the overall emission estimate.

Generally, the PBLH was well defined and was detected from the maximum in the gradient or manually from potential temperature, water vapor mixing ratio and vertical wind during profile flights before or after the mass balance flight pattern. An example is shown in Figure A2.

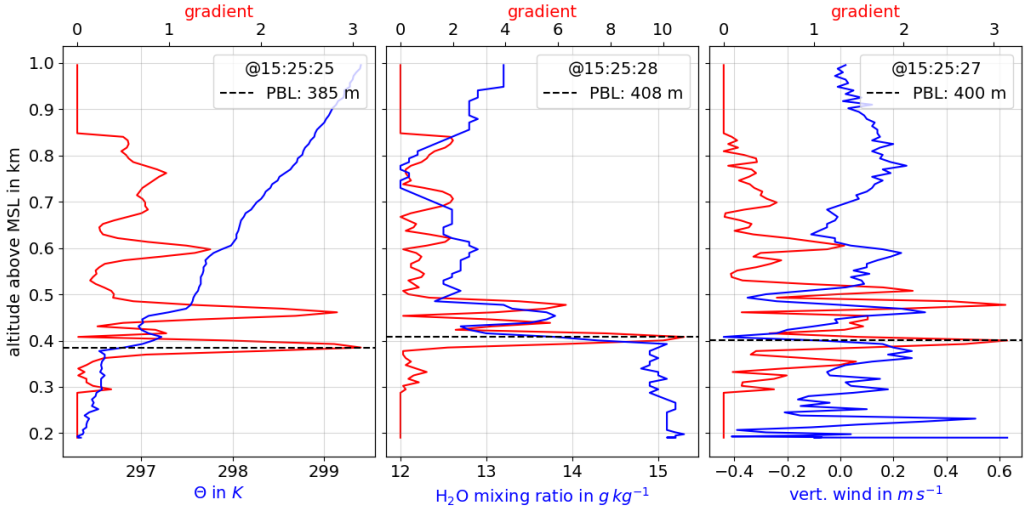

Figure A2: PBLH determination from gradients in potential temperature Θ, water vapor mixing ratio and vertical wind for one profile during flight 13b.

https://doi.org/10.5194/egusphere-2025-635
Preprint. Discussion started: 21 February 2025

The theoretically lowest detectable flux was defined as the smallest signal detectable with 95% significance (2σ) over three consecutive time steps in each transect of the mass balance calculation. The final lowest detectable flux is then the sum of the lowest detectable fluxes across all transects. This threshold is primarily influenced by measurement and background uncertainties: if background variation exceeds measurement uncertainty, signal enhancements remain undetectable, precluding flux calculations. Wind speed and PBLH are also factored in, as they affect plume mixing within the boundary layer. The calculated lowest detectable fluxes are between 0.8 and 10.3 kg h^{-1} CH_4 and between 406 and 7116 kg h^{-1} CO_2. The lowest values occurred for one measurement close to the coast, where the wind speed was only 1.3 m s^{-1}, the background concentration uncertainty at 0.96 ppb CH_4 and 0.04 ppm CO_2. The observed enhancement in this case was 10 ppb CH_4 and 0.40 ppm CO_2, resulting in a flux of 27 kg h^{-1} CH_4 and 2430 kg h^{-1} CO_2 at 340 m PBLH. For CO_2, this is close to the instrument uncertainty, but due to the low background concentration uncertainty, the plume is clearly distinguishable and counted. In other cases, the CO_2 background is more variable and plumes cannot be clearly distinguished. Of the total 85 mass balances, 9 were below the detectable flux for CH_4 and 13 for CO_2.

Appendix B: CO_2 gridded emission inventories

Figure B1 shows the CO_2 emission distribution of EDGAR v8.0 and CAMS v5.3 for the year 2022. This distribution matches well with the location of the offshore facilities.

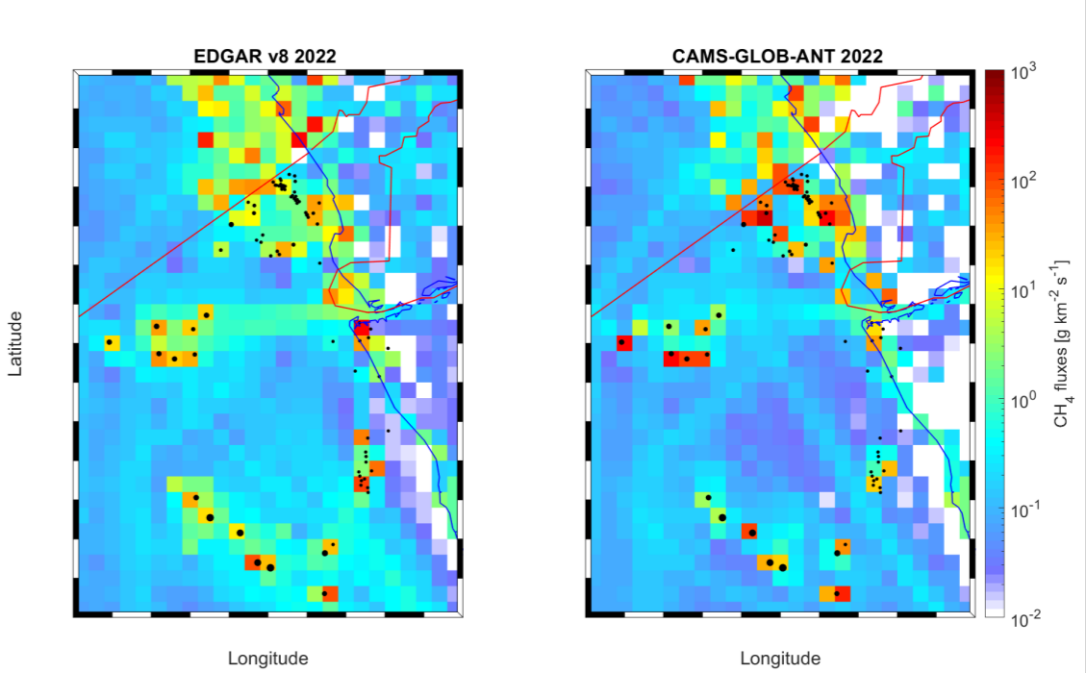

Figure B1: Maps of annual CO_2 emissions for the year 2022 from the two emission inventories EDGAR v8.0 and CAMS-GLOB-ANT v5.3.

https://doi.org/10.5194/egusphere-2025-635
Preprint. Discussion started: 21 February 2025

Author contributions: Alina Fiehn prepared the campaign, collected, analyzed, and interpreted the data and wrote the manuscript. Maximilian Eckl coordinated the measurements during the campaign phase and developed the mass balance routine. Tiziana Bräuer and Magdalena Pühl measured and analyzed the CH_4, CO_2, CO, NO_y and C_2H_6 data. Klaus-Dirk Gottschaldt led the weather forecast, flight planning and execution operations. Heinfried Aufmhoff and Lisa Eirenschmalz measured and analyzed SO_2. Gregor Neumann, Felicitas Sakellariou, and Daniel Sauer measured and analyzed the aerosol data. Guilherme De Aguiar Ventura, Winne Nayole Cadete, Dario Luciano Zua, Manuel Xavier, Paulo Correia led communication with the operators, collected and provided their data and helped interpreting it. Anke Roiger developed the research idea and led the MTGA project. All authors contributed to the interpretation of the results and the improvement of the manuscript.

Competing interests: The authors have no competing interests.

Acknowledgement: The authors thank DLR-FX for the campaign cooperation, especially the pilots Michael Grossrubatscher and Götz Hieber, in-flight technicians David Woudsma and Georg Reiser, the sensor group of Andreas Giez, Martin Zöger, Kevin Raynor and Andreas Numberger, project manager Oliver Paxa, flight operations officer Frank Probst, technicians Stephan Storhas and Robert Uebelacker. We also thank Larissa Mengue and Mpiga Assele Ulrich from the Agence Gabonese d'Etudes aet d'Observations Spatiales (AGEOS) for their support of the campaign at our base in Gabon, the Gabonese Airforce for the opportunity to use their Libreville facilities for our flight operations.

Funding information: This project has been funded through UNEP's International Methane Emissions Observatory (IMEO).

Data accessibility: The measurement data is stored on the HALO database (https://halo-db.pa.op.dlr.de/) and publicly available at zenodo (Fiehn et al., 2025).

https://doi.org/10.5194/egusphere-2025-635
Preprint. Discussion started: 21 February 2025

References

Bramberger, M., Dörnbrack, A., Bossert, K., Ehard, B., Fritts, D. C., Kaifler, B., Mallaun, C., Orr, A., Pautet, P.-D., Rapp, M., Taylor, M. J., Vosper, S., Williams, B. P., and Witschas, B.: Does Strong Tropospheric Forcing Cause Large-Amplitude Mesospheric Gravity Waves? A DEEPWAVE Case Study, Journal of Geophysical Research: Atmospheres, 122, 11,422-411,443, https://doi.org/10.1002/2017JD027371, 2017.

Cain, M., Warwick, N. J., Fisher, R. E., Lowry, D., Lanoisellé, M., Nisbet, E. G., France, J., Pitt, J., O'Shea, S., Bower, K. N., Allen, G., Illingworth, S., Manning, A. J., Bauguitte, S., Pisso, I., and Pyle, J. A.: A cautionary tale: A study of a methane enhancement over the North Sea, Journal of Geophysical Research: Atmospheres, 122, 7630-7645, https://doi.org/10.1002/2017JD026626, 2017.

Conley, S., Franco, G., Faloona, I., Blake, D. R., Peischl, J., and Ryerson, T. B.: Methane emissions from the 2015 Aliso Canyon blowout in Los Angeles, CA, Science, 351, 1317-1320, doi:10.1126/science.aaf2348, 2016.

Dischl, R. K., Sauer, D., Voigt, C., Harlaß, T., Sakellariou, F., Märkl, R. S., Schumann, U., Scheibe, M., Kaufmann, S., Roiger, A., Dörnbrack, A., Renard, C., Gauthier, M., Swann, P., Madden, P., Luff, D., Johnson, M., Ahrens, D., Sallinen, R., Schripp, T., Eckel, G., Bauder, U., and Le Clercq, P.: Measurements of particle emissions of an A350-941 burning 100% sustainable aviation fuels in cruise, EGUsphere, 2024, 1-29, 10.5194/egusphere-2024-1224, 2024.

European Comission JRC: EDGAR Methodology, https://edgar.jrc.ec.europa.eu/methodology, access: 26.07.2024, 2024.

European Commission, and United States of America: Global Methan Pledge, Glasgow, Scotland, https://www.globalmethanepledge.org/, 2021.

European Commission JRC: EDGAR v8.0, Global Greenhouse Gas Emissions, https://edgar.jrc.ec.europa.eu/dataset_ghg80, access: 26.07.2024, 2024.

Feldpausch, P., Fiebig, M., Fritzsche, L., and Petzold, A.: Measurement of ultrafine aerosol size distributions by a combination of diffusion screen separators and condensation particle counters, Journal of Aerosol Science, 37, 577-597, https://doi.org/10.1016/j.jaerosci.2005.04.009, 2006.

Fiehn, A., Kostinek, J., Eckl, M., Klausner, T., Gałkowski, M., Chen, J., Gerbig, C., Röckmann, T., Maazallahi, H., Schmidt, M., Korbeń, P., Nęçki, J., Jagoda, P., Wildmann, N., Mallaun, C., Bun, R., Nickl, A. L., Jöckel, P., Fix, A., and Roiger, A.: Estimating CH4, CO2 and CO emissions from coal mining and industrial activities in the Upper Silesian Coal Basin using an aircraft-based mass balance approach, Atmos. Chem. Phys., 20, 12675-12695, 10.5194/acp-20-12675-2020, 2020.

Fiehn, A., Roiger, A., Eckl, M., Pühl, M., Bräuer, T., Gottschaldt, K.-D., Aufmhoff, H., Eirenschmalz, L., Neumann, G., Sakellariou, F., and Sauer, D.: Airborne observation data from the METHANE-To-Go Africa campaign in September 2022, 5, https://doi.org/10.5281/zenodo.14849611, 2025.

Fimpel, H. P.: The DLR Meteorological Research Aircraft FALCON, DLR, https://elib.dlr.de/63837/1/91-fmpl.pdf, 1991.

Foulds, A., Allen, G., Shaw, J. T., Bateson, P., Barker, P. A., Huang, L., Pitt, J. R., Lee, J. D., Wilde, S. E., Dominutti, P., Purvis, R. M., Lowry, D., France, J. L., Fisher, R. E., Fiehn, A., Pühl, M., Bauguitte, S. J. B., Conley, S. A., Smith, M. L., Lachlan-Cope, T., Pisso, I., and Schwietzke, S.: Quantification and assessment of methane emissions from offshore oil and gas facilities on the Norwegian continental shelf, Atmos. Chem. Phys., 22, 4303-4322, 10.5194/acp-22-4303-2022, 2022.

Giez, A., Zöger, M., Mallaun, C., Nenakhov, V., Schimpf, M., Grad, C., Numberger, A., and Raynor, K.: Determination of the Measurement Errors for the HALO Basic Data System BAHAMAS by Means of Error Propagation, Deutsches Zentrum für Luft- und Raumfahrt, Oberpfaffenhofen, 1434-8454, https://doi.org/10.57676/5rdc-q708, 2022.

Gorchov Negron, A. M., Kort, E. A., Chen, Y., Brandt, A. R., Smith, M. L., Plant, G., Ayasse, A. K., Schwietzke, S., Zavala-Araiza, D., Hausman, C., and Adames-Corraliza, Á. F.: Excess methane emissions from shallow water platforms elevate the carbon intensity of US Gulf of Mexico oil and gas production, Proceedings of the National Academy of Sciences, 120, e2215275120, 10.1073/pnas.2215275120, 2023.

Granier, C., Darras, S., Denier van der Gon, H., Doubalova, J., Elguindi, N., Galle, B., Gauss, M., Guevara, M., Jalkanen, J.-P., Kuenen, J., Liousse, C., Quack, B., Simpson, D., and Sindelarova, K.: The Copernicus Atmosphere Monitoring Service global and regional emissions (April 2019 version), Copernicus Atmosphere Monitoring Service (CAMS), 10.24380/d0bn-kx16, 2019.

Harlass, T., Dischl, R., Kaufmann, S., Märkl, R., Sauer, D., Scheibe, M., Stock, P., Bräuer, T., Dörnbrack, A., Roiger, A., Schlager, H., Schumann, U., Schripp, T., Grein, T., Bondorf, L., Renard, C., Gauthier, M., Johnson, M., Luff, D., Madden, P., Swann, P., Ahrens, D., Sallinen, R., and Voigt, C.: Measurement report: In-flight and ground-based measurements of nitrogen oxide emissions from latest generation jet engines and 100% sustainable aviation fuel, EGUsphere, 2024, 1-22, 10.5194/egusphere-2024-454, 2024.

Hensen, A., Velzeboer, I., Frumau, K. F. A., Bulk, W. C. M. v. d., and Dinther, D. v.: Methane emission measurements of offshore oil and gas platforms, TNO, Petten, Netherlands, https://resolver.tno.nl/uuid:a9c705b9-ec88-4316-827f-f9d7ffbd05c2, 94, 2019.

IEA: Methane Tracker, https://www.iea.org/data-and-statistics/data-tools/methane-tracker, access: 07.06.2024, 2024.

https://doi.org/10.5194/egusphere-2025-635
Preprint. Discussion started: 21 February 2025

IPCC: Climate Change 2021: The Physical Science Basis. Contribution of Working Group I to the Sixth Assessment Report of the Intergovernmental Panel on Climate Change, edited by: Masson-Delmotte, V., Zhai, P., Pirani, A., Connors, S. L., Péan, C., Berger, S., Caud, N., Chen, Y., Goldfarb, L., Gomis, M. I., Huang, M., Leitzell, K., Lonnoy, E., Matthews, J. B. R., Maycock, T. K., Waterfield, T., Yelekçi, O., Yu, R., and Zhou, B., Cambridge University Press, Cambridge, United Kingdom and New York, NY, USA, 2021.

IPCC: The Earth's Energy Budget, Climate Feedbacks and Climate Sensitivity, in: Climate Change 2021 – The Physical Science Basis: Working Group I Contribution to the Sixth Assessment Report of the Intergovernmental Panel on Climate Change, edited by: Intergovernmental Panel on Climate, C., Cambridge University Press, Cambridge, 923-1054, 2023.

Karion, A., Sweeney, C., Wolter, S., Newberger, T., Chen, H., Andrews, A., Kofler, J., Neff, D., and Tans, P.: Long-term greenhouse gas measurements from aircraft, Atmos. Meas. Tech., 6, 511-526, 10.5194/amt-6-511-2013, 2013.

Klausner, T.: Aircraft-based in situ measurements of CH4 and CO2 downstream of European and Asian urban centres at local to synoptic scales, Dr. rer. nat., Fakultät für Physik, Ludwig-Maximilians-Universität München, Munich, Germany, 173, pp., 10.5282/edoc.26983, 2020.

Kostinek, J., Roiger, A., Davis, K. J., Sweeney, C., DiGangi, J. P., Choi, Y., Baier, B., Hase, F., Groß, J., Eckl, M., Klausner, T., and Butz, A.: Adaptation and performance assessment of a quantum and interband cascade laser spectrometer for simultaneous airborne in situ observation of CH4, C2H6, CO2, CO and N2O, Atmos. Meas. Tech., 12, 1767-1783, 10.5194/amt-12-1767-2019, 2019.

Lee, J. D., Mobbs, S. D., Wellpott, A., Allen, G., Bauguitte, S. J. B., Burton, R. R., Camilli, R., Coe, H., Fisher, R. E., France, J. L., Gallagher, M., Hopkins, J. R., Lanoiselle, M., Lewis, A. C., Lowry, D., Nisbet, E. G., Purvis, R. M., O'Shea, S., Pyle, J. A., and Ryerson, T. B.: Flow rate and source reservoir identification from airborne chemical sampling of the uncontrolled Elgin platform gas release, Atmos. Meas. Tech., 11, 1725-1739, 10.5194/amt-11-1725-2018, 2018.

Luke, W. T.: Evaluation of a commercial pulsed fluorescence detector for the measurement of low-level SO2 concentrations during the Gas-Phase Sulfur Intercomparison Experiment, Journal of Geophysical Research: Atmospheres, 102, 16255-16265, https://doi.org/10.1029/96JD03347, 1997.

Lyon, D. R., Zavala-Araiza, D., Alvarez, R. A., Harriss, R., Palacios, V., Lan, X., Talbot, R., Lavoie, T., Shepson, P., Yacovitch, T. I., Herndon, S. C., Marchese, A. J., Zimmerle, D., Robinson, A. L., and Hamburg, S. P.: Constructing a Spatially Resolved Methane Emission Inventory for the Barnett Shale Region, Environmental Science & Technology, 49, 8147-8157, 10.1021/es506359c, 2015.

MacKay, K., Lavoie, M., Bourlon, E., Atherton, E., O'Connell, E., Baillie, J., Fougère, C., and Risk, D.: Methane emissions from upstream oil and gas production in Canada are underestimated, Scientific Reports, 11, 8041, 10.1038/s41598-021-87610-3, 2021.

Masnadi, M. S., El-Houjeiri, H. M., Schunack, D., Li, Y., Englander, J. G., Badahdah, A., Monfort, J.-C., Anderson, J. E., Wallington, T. J., Bergerson, J. A., Gordon, D., Koomey, J., Przesmitzki, S., Azevedo, I. L., Bi, X. T., Duffy, J. E., Heath, G. A., Keoleian, G. A., McGlade, C., Meehan, D. N., Yeh, S., You, F., Wang, M., and Brandt, A. R.: Global carbon intensity of crude oil production, Science, 361, 851-853, doi:10.1126/science.aar6859, 2018.

Mays, K. L., Shepson, P. B., Stirm, B. H., Karion, A., Sweeney, C., and Gurney, K. R.: Aircraft-Based Measurements of the Carbon Footprint of Indianapolis, Environmental Science & Technology, 43, 7816-7823, 10.1021/es901326b, 2009.

Nara, H., Tanimoto, H., Tohjima, Y., Mukai, H., Nojiri, Y., and Machida, T.: Emissions of methane from offshore oil and gas platforms in Southeast Asia, Scientific Reports, 4, 6503, 10.1038/srep06503, 2014.

Nisbet, E. G., Manning, M. R., Dlugokencky, E. J., Fisher, R. E., Lowry, D., Michel, S. E., Myhre, C. L., Platt, S. M., Allen, G., Bousquet, P., Brownlow, R., Cain, M., France, J. L., Hermansen, O., Hossaini, R., Jones, A. E., Levin, I., Manning, A. C., Myhre, G., Pyle, J. A., Vaughn, B. H., Warwick, N. J., and White, J. W. C.: Very Strong Atmospheric Methane Growth in the 4 Years 2014–2017: Implications for the Paris Agreement, Global Biogeochemical Cycles, 33, 318-342, 10.1029/2018GB006009, 2019.

Pandey, S., Gautam, R., Houweling, S., van der Gon, H. D., Sadavarte, P., Borsdorff, T., Hasekamp, O., Landgraf, J., Tol, P., van Kempen, T., Hoogeveen, R., van Hees, R., Hamburg, S. P., Maasakkers, J. D., and Aben, I.: Satellite observations reveal extreme methane leakage from a natural gas well blowout, Proceedings of the National Academy of Sciences, 116, 26376-26381, 10.1073/pnas.1908712116, 2019.

Pitt, J. R., Allen, G., Bauguitte, S. J. B., Gallagher, M. W., Lee, J. D., Drysdale, W., Nelson, B., Manning, A. J., and Palmer, P. I.: Assessing London CO2, CH4 and CO emissions using aircraft measurements and dispersion modelling, Atmos. Chem. Phys., 19, 8931-8945, 10.5194/acp-19-8931-2019, 2019.

Pühl, M., Roiger, A., Fiehn, A., Gorchov Negron, A. M., Kort, E. A., Schwietzke, S., Pisso, I., Foulds, A., Lee, J., France, J. L., Jones, A. E., Lowry, D., Fisher, R. E., Huang, L., Shaw, J., Bateson, P., Andrews, S., Young, S., Dominutti, P., Lachlan-Cope, T., Weiss, A., and Allen, G.: Aircraft-based mass balance estimate of methane emissions from offshore gas facilities in the southern North Sea, Atmos. Chem. Phys., 24, 1005-1024, 10.5194/acp-24-1005-2024, 2024.

Republic of Angola: Second National Communication, Ministry of Culture, Tourism and Environment, Luanda, Angola, 330, 2021.

https://doi.org/10.5194/egusphere-2025-635
Preprint. Discussion started: 21 February 2025

Riddick, S. N., Mauzerall, D. L., Celia, M., Harris, N. R. P., Allen, G., Pitt, J., Staunton-Sykes, J., Forster, G. L., Kang, M., Lowry, D., Nisbet, E. G., and Manning, A. J.: Methane emissions from oil and gas platforms in the North Sea, Atmos. Chem. Phys., 19, 9787-9796, 10.5194/acp-19-9787-2019, 2019.

Roiger, A., Thomas, J. L., Schlager, H., Law, K. S., Kim, J., Schäfler, A., Weinzierl, B., Dahlkötter, F., Krisch, I., Marelle, L., Minikin, A., Raut, J. C., Reiter, A., Rose, M., Scheibe, M., Stock, P., Baumann, R., Bouarar, I., Clerbaux, C., George, M., Onishi, T., and Flemming, J.: Quantifying Emerging Local Anthropogenic Emissions in the Arctic Region: The ACCESS Aircraft Campaign Experiment, Bulletin of the American Meteorological Society, 96, 441-460, https://doi.org/10.1175/BAMS-D-13-00169.1, 2015.

Saunois, M., Stavert, A. R., Poulter, B., Bousquet, P., Canadell, J. G., Jackson, R. B., Raymond, P. A., Dlugokencky, E. J., Houweling, S., Patra, P. K., Ciais, P., Arora, V. K., Bastviken, D., Bergamaschi, P., Blake, D. R., Brailsford, G., Bruhwiler, L., Carlson, K. M., Carrol, M., Castaldi, S., Chandra, N., Crevoisier, C., Crill, P. M., Covey, K., Curry, C. L., Etiope, G., Frankenberg, C., Gedney, N., Hegglin, M. I., Höglund-Isaksson, L., Hugelius, G., Ishizawa, M., Ito, A., Janssens-Maenhout, G., Jensen, K. M., Joos, F., Kleinen, T., Krummel, P. B., Langenfelds, R. L., Laruelle, G. G., Liu, L., Machida, T., Maksyutov, S., McDonald, K. C., McNorton, J., Miller, P. A., Melton, J. R., Morino, I., Müller, J., Murguia-Flores, F., Naik, V., Niwa, Y., Noce, S., O'Doherty, S., Parker, R. J., Peng, C., Peng, S., Peters, G. P., Prigent, C., Prinn, R., Ramonet, M., Regnier, P., Riley, W. J., Rosentreter, J. A., Segers, A., Simpson, I. J., Shi, H., Smith, S. J., Steele, L. P., Thornton, B. F., Tian, H., Tohjima, Y., Tubiello, F. N., Tsuruta, A., Viovy, N., Voulgarakis, A., Weber, T. S., van Weele, M., van der Werf, G. R., Weiss, R. F., Worthy, D., Wunch, D., Yin, Y., Yoshida, Y., Zhang, W., Zhang, Z., Zhao, Y., Zheng, B., Zhu, Q., Zhu, Q., and Zhuang, Q.: The Global Methane Budget 2000–2017, Earth Syst. Sci. Data, 12, 1561-1623, 10.5194/essd-12-1561-2020, 2020.

Scarpelli, T. R., Jacob, D. J., Maasakkers, J. D., Sulprizio, M. P., Sheng, J. X., Rose, K., Romeo, L., Worden, J. R., and Janssens-Maenhout, G.: A global gridded (0.1° × 0.1°) inventory of methane emissions from oil, gas, and coal exploitation based on national reports to the United Nations Framework Convention on Climate Change, Earth Syst. Sci. Data, 12, 563-575, 10.5194/essd-12-563-2020, 2020.

Scarpelli, T. R., Jacob, D. J., Grossman, S., Lu, X., Qu, Z., Sulprizio, M. P., Zhang, Y., Reuland, F., Gordon, D., and Worden, J. R.: Updated Global Fuel Exploitation Inventory (GFEI) for methane emissions from the oil, gas, and coal sectors: evaluation with inversions of atmospheric methane observations, Atmos. Chem. Phys., 22, 3235-3249, 10.5194/acp-22-3235-2022, 2022.

Schwietzke, S., Sherwood, O. A., Bruhwiler, L. M. P., Miller, J. B., Etiope, G., Dlugokencky, E. J., Michel, S. E., Arling, V. A., Vaughn, B. H., White, J. W. C., and Tans, P. P.: Upward revision of global fossil fuel methane emissions based on isotope database, Nature, 538, 88, 10.1038/nature19797, 2016.

Shen, L., Jacob, D. J., Gautam, R., Omara, M., Scarpelli, T. R., Lorente, A., Zavala-Araiza, D., Lu, X., Chen, Z., and Lin, J.: National quantifications of methane emissions from fuel exploitation using high resolution inversions of satellite observations, Nature Communications, 14, 4948, 10.1038/s41467-023-40671-6, 2023.

Soulie, A., Granier, C., Darras, S., Zilbermann, N., Doumbia, T., Guevara, M., Jalkanen, J. P., Keita, S., Liousse, C., Crippa, M., Guizzardi, D., Hoesly, R., and Smith, S.: Global Anthropogenic Emissions (CAMS-GLOB-ANT) for the Copernicus Atmosphere Monitoring Service Simulations of Air Quality Forecasts and Reanalyses, Earth Syst. Sci. Data Discuss., 2023, 1-45, 10.5194/essd-2023-306, 2023.

Speidel, M., Nau, R., Arnold, F., Schlager, H., and Stohl, A.: Sulfur dioxide measurements in the lower, middle and upper troposphere: Deployment of an aircraft-based chemical ionization mass spectrometer with permanent in-flight calibration, Atmospheric Environment, 41, 2427-2437, https://doi.org/10.1016/j.atmosenv.2006.07.047, 2007.

Turnbull, J. C., Karion, A., Fischer, M. L., Faloona, I., Guilderson, T., Lehman, S. J., Miller, B. R., Miller, J. B., Montzka, S., Sherwood, T., Saripalli, S., Sweeney, C., and Tans, P. P.: Assessment of fossil fuel carbon dioxide and other anthropogenic trace gas emissions from airborne measurements over Sacramento, California in spring 2009, Atmos. Chem. Phys., 11, 705-721, 10.5194/acp-11-705-2011, 2011.

UNEP: IMEO Methane Data, https://methanedata.unep.org, access: 24.05.2024, 2024.

UNFCCC: Adoption of the Paris Agreement, Conference of the Parties: Twenty-first session, Paris, France, 30 November–13 December 2015, 2015.

UNFCCC: Greenhouse Gas Inventory Data - Detailed data by Party, https://di.unfccc.int/, 2023.

Varon, D. J., McKeever, J., Jervis, D., Maasakkers, J. D., Pandey, S., Houweling, S., Aben, I., Scarpelli, T., and Jacob, D. J.: Satellite Discovery of Anomalously Large Methane Point Sources From Oil/Gas Production, Geophysical Research Letters, 46, 13507-13516, 10.1029/2019gl083798, 2019.

Xiao, Y., Logan, J. A., Jacob, D. J., Hudman, R. C., Yantosca, R., and Blake, D. R.: Global budget of ethane and regional constraints on U.S. sources, Journal of Geophysical Research: Atmospheres, 113, 10.1029/2007jd009415, 2008.

Yacovitch, T. I., Daube, C., and Herndon, S. C.: Methane Emissions from Offshore Oil and Gas Platforms in the Gulf of Mexico, Environmental Science & Technology, 54, 3530-3538, 10.1021/acs.est.9b07148, 2020.

Zavala-Araiza, D., Alvarez, R. A., Lyon, D. R., Allen, D. T., Marchese, A. J., Zimmerle, D. J., and Hamburg, S. P.: Super-emitters in natural gas infrastructure are caused by abnormal process conditions, Nature Communications, 8, 14012, 10.1038/ncomms14012, 2017.